Semiclassical instanton approach to calculation of reaction rate constants in multidimensional chemical systems

Maksym Kryvohuz[a)]
Arthur Amos Noyes Laboratory of Chemical Physics, 127-72, California Institute of Technology, Pasadena, California 91125, USA

(Received 29 October 2010; accepted 23 February 2011; published online 17 March 2011)

The semiclassical instanton approximation is revisited in the context of its application to the calculation of chemical reaction rate constants. An analytical expression for the quantum canonical reaction rate constants of multidimensional systems is derived for all temperatures from the deep tunneling to high-temperature regimes. The connection of the derived semiclassical instanton theory with several previously developed reaction rate theories is shown and the numerical procedure for the search of instanton trajectories is provided. The theory is tested on seven different collinear symmetric and asymmetric atom transfer reactions including heavy-light-heavy, light-heavy-light and light-light-heavy systems. The obtained thermal rate constants agree within a factor of 1.5–2 with the exact quantum results in the wide range of temperatures from 200 to 1500 K. © *2011 American Institute of Physics*. [doi:10.1063/1.3565425]

I. INTRODUCTION

The calculation of canonical reaction rate constants is an important task of theoretical chemistry. For electronically adiabatic chemical reactions, the latter problem can be considered as the problem of probability decay of metastable nuclear states of reactants on electronically adiabatic potential energy surface (PES). At high temperatures the escape rate from metastable reactant states is that of activated barrier crossing and can be well described by means of classical mechanical theories such as transition state theory (TST). At low temperatures, over- the- barrier mechanisms of escape from a metastable well are minor and under-the-barrier quantum tunneling escape mechanism becomes dominant. The incorporation of both mechanisms are important for correct description of quantum chemical reaction rates at all temperatures.

The unified theory that rigorously incorporates classically allowed as well as quantum tunneling rate mechanisms has been developed in the past[1,2] and the smooth connection between the low-temperature and high-temperature reaction rate regimes was shown for dissipative[3,4] and nondissipative[1,2] onedimensional systems. Yet, for nonseparable multidimensional systems the development of the unified reaction rate theory is not a trivial task. The latter is due to the fact that quantum tunneling mechanism is not obvious in the case of multidimensional systems. While in one dimensional systems quantum tunneling effects can be accounted for by using WKB approximation along the tunneling path, in multiple dimensions the concept of "tunneling path" is ambiguous. Several tunneling paths have been suggested in the past based on physical intuition to incorporate multidimensional quantum tunneling effects into reaction rate theory.[5,6] Yet, the latter tunneling paths are introduced in the form of *ad hoc* corrections and therefore are not rigorous.

The semiclassical instanton (SI) approximation introduced by Miller in Ref. 7 provided a way for rigorous semiclassical description of tunneling effects in many-dimensional nonseparable systems. Since then, the semiclassical instanton approach has been widely used in low temperature physics to describe tunnel splittings of ground state energy levels in polyatomic systems,[8–11] to calculate lifetimes of multidimensional metastable states[11] and to study the effects of dissipation on quantum tunneling.[12–14] SI approximation requires neither *ad hoc* tunneling paths nor separability of PES, but instead uses the particular path determined by classical dynamics on the full potential surface. It also correctly accounts for corner cutting quantum effects as well as naturally incorporates zero-point energy quantization by calculating stability frequencies along the tunneling path. In fact, for applications of low temperature physics the semiclassical instanton approximation was shown to be a rigorous semiclassical limit of quantum mechanics, accurate to first order in Planck's constant $\hbar$.[11] Some recent developments in the instanton theory include free energy version of instanton approach,[15] harmonic quantum transition state theory,[16] and the connection of instanton approach to the ring polymer molecular dynamics method.[17]

Yet, while SI approximation works very well for one-dimensional systems and low-temperature multidimensional systems, its application to multidimensional chemical systems at the temperatures of general interest showed poor agreement with exact quantum results.[18] There were three major problems with semiclassical instanton rate theory. The first issue was that the semiclassical instanton rate theory did not provide an expression for reaction rate coefficient at temperatures above the critical temperature, which is the temperature of vanishing of instantons and its magnitude is in the range of room temperatures for many chemical systems. The second issue was the poor agreement even of low-temperature semiclassical instanton results with the corresponding

a)Electronic mail: maximian@caltech.edu.

exact quantum results, which therefore required an *ad hoc* correction discussed in Ref. 18. And the third issue was the difficulty of locating periodic trajectories on general potential energy surfaces. These issues were probably the reason for low interest of chemical community in the semiclassical instanton theory.

The purpose of the present paper is to fix the problems of SI approximation that prevented its applications in chemical physics. We revisit the derivation of SI rate constant starting with the imaginary free energy approach to reaction rate theory. We then provide SI expressions of rate constants valid in the whole temperature range by reducing the original multidimensional problem to the effective one-dimensional problem and employing the well developed apparatus of one-dimensional approximation methods. We also provide a practical method for the search of instanton trajectories. We argue that, with the improvements been made, the semiclassical instanton theory becomes quantitative and provides approximate canonical rate constants that agree with the exact quantum results within the factor of no more than 1.5–2 in the temperature range 150–1500 K. While modern quantum numerical methods[19,20] can provide more accurate approximation of rate constants, the SI approximation discussed in the present paper is analytical, transparent, and physically intuitive, which therefore allows physical insight about tunneling dynamics as well as the contribution of tunneling to reaction rates.

The paper is organized as follows. In Secs. II–III we review the derivation of SI theory from the imaginary free energy approach and in Sec. IV derive rate constant expressions for the simplest version of SI approximation, which we call SI1 approximation. In Sec. V we show the connection of the derived rate constant expressions with those of other rate theories. In Sec. VI we provide a slightly improved SI approximation for reaction rate constants, which we call SI2 approximation. We propose a method for practical implication of semiclassical instanton SI1 and SI2 approximations in Sec. VII and provide numerical results for seven different collinear reactions in Sec. VIII. We conclude with discussions in Sec. IX.

II. IMAGINARY FREE ENERGY APPROACH TO REACTION RATE CONSTANTS

To obtain an expression for reaction rate coefficients we use the approach based on the relationship between the rate of decay of a metastable state and the imaginary part of system's free energy.[1,8,21] Any chemical reaction, for which one can define a concept of rate, is equivalent to the process of decay of its reactant states, which therefore can be considered as metastable states. In principle, not all chemical processes can be described with a rate. For instance, for the process of coherent tunneling in a symmetric double-well potential, in which a particle initially localized in the left well tunnels to the right well at later times, one cannot ascribe a rate constant since this process is reversible. In the latter case the probability of finding particle in the left well periodically oscillates with time[22] instead of decaying exponentially. In the present paper we consider only those chemical reactions for which the decay of reactants is clear and the coherence effects (recrossings) are minor so that the concept of rate can be introduced. The same assumption of minor recrossings is present in another well-established theory of chemical reaction rates, the transition state theory,[7] which assumes only one-way direction of reactive flux at the transition state.

If the rate of escape from some metastable state is Γ_n then the energy level of this metastable state is broadened with the width Γ_n and can be represented in complex form $E_n = E_{0n} - (\imath\Gamma_n\hbar)/2$. Ref. 23 where E_{0n} is real and corresponds to the energy of the state in the absence of escape. The time evolution of this metastable state given by the factor $\exp(-\imath E_n t/\hbar)$, therefore, results in the exponential decay of the probability to remain in this state $|\Psi_n|^2 \sim \exp(-\Gamma_n t)$. Thus, the escape rate from a metastable level can be represented as the imaginary part of its energy

$$\Gamma_n = -\frac{2}{\hbar}\mathrm{Im}E_n. \tag{1}$$

For a canonical ensemble of temperature T one should take a Boltzmann average of the Eq. (1) resulting in Ref. 1

$$k = -\frac{2}{\hbar}\mathrm{Im}F, \tag{2}$$

where k is a canonical rate constant and F is a free energy. The relationship between the rate of escape and the imaginary part of system's free energy is known in both quantum and classical mechanics,[1] since metastability of a state can be of pure quantum origin due to tunneling escape mechanism or of classical origin due to thermally activated barrier crossing mechanism. The connection between these two limits has been extensively studied in the past.[3,4]

Using the well-known relation between free energy and partition function, $F = -\beta^{-1}\ln Q$, where $\beta \equiv 1/\kappa_B T$ and Q is system's partition function, one obtains

$$\begin{aligned} k &= \frac{2}{\hbar\beta}\mathrm{Im}\left(\ln Q\right), \\ &= \frac{2}{\hbar\beta}\arctan\left(\frac{\mathrm{Im}Q}{\mathrm{Re}Q}\right), \\ &= \frac{2}{\hbar\beta}\frac{\mathrm{Im}Q}{\mathrm{Re}Q}, \end{aligned} \tag{3}$$

since $\mathrm{Im}Q \ll \mathrm{Re}Q$. Equation (3) expresses the main idea of the imaginary free energy approach, it relates thermal rate constant to the imaginary part of partition function.[24] The relation between the imaginary part of partition function and the reactive flux correlation function has also been shown in Ref. 2, and the possibility to express the exact quantum mechanical reaction rate in terms of the Siegert eigenvalues (the complex eigenvalues of the Schrodinger equation) has been discussed in Ref. 25.

The origin of the imaginary part of partition function can be seen from the following simple example. The partition function of a harmonic potential well is known to be $Q_{h.o.} = [2\sinh(\beta\omega\hbar/2)]^{-1}$. The partition function of a harmonic barrier can be obtained by flipping the harmonic potential well, i.e., by replacing ω with $\imath\omega$. One thus obtains the partition function of a harmonic barrier by analytical continuation $Q_{h.barr.} = [\imath 2\sin(\beta\omega\hbar/2)]^{-1}$, which is pure

imaginary. Since any multidimensional potential barrier of a chemical system has exactly one unstable mode, the one that corresponds to the reaction coordinate, so the partition function of a multidimensional barrier, which in the separable limit is a product of partition functions of each mode is pure imaginary.[26] A multidimensional potential well, instead, has only stable modes and thus its partition function is pure real. General potential energy surfaces of chemical systems have both stable (minimums) and unstable (barriers) extremums, therefore their partition functions always have real as well as imaginary parts.

We now review the derivation of the semiclassical expression of partition function following the rigorous derivations of Benderskii *et al.* in the Refs. 8, 27, and 28. Partition function Q is given as a trace of the Boltzmann operator, which in coordinate representation reads[29,30]

$$Q = \int d\mathbf{x} \, \langle \mathbf{x} | \, e^{-\beta H} \, | \mathbf{x} \rangle \, , \tag{4}$$

where $\mathbf{x}$ is N-dimensional vector corresponding to N degrees of freedom. Everywhere in the paper we use mass-scales coordinates $\mathbf{x}_i = \sqrt{m_i}\mathbf{q}_i$. The latter reduces the original N-dimensional many-body problem to the effective problem of a single particle of unitary mass in N-dimensional space. Introducing complex time $t \equiv -\imath\hbar\beta$ and using path-integral representation[29] of the propagator $\langle \mathbf{x}_i | e^{-\imath H t/\hbar} | \mathbf{x}_f \rangle = \int D[\mathbf{x}(\tau)] e^{-\imath S[\mathbf{x}(\tau)]/\hbar}$ one gets the well known expression of the partition function[29]

$$Q = \oint D[\mathbf{x}(\tau)] e^{-S[\mathbf{x}(\tau)]/\hbar}, \tag{5}$$

where $S[\mathbf{x}(\tau)]$ is Euclidian action on the inverted potential $-V(\mathbf{x})$

$$S[\mathbf{x}(\tau)] = \int_0^{\hbar\beta} \left[\frac{1}{2} \left(\frac{d\mathbf{x}}{d\tau} \right)^2 + V(\mathbf{x}(\tau)) \right] d\tau, \tag{6}$$

and the path integral $\oint \equiv \int d\mathbf{x}_i \int_{\mathbf{x}(0)=\mathbf{x}_i}^{\mathbf{x}(\hbar\beta)=\mathbf{x}_i}$ in Eq. (5) is taken over the closed paths $\mathbf{x}(0) = \mathbf{x}(\hbar\beta) = \mathbf{x}_i$. The effective inversion of potential $V(\mathbf{x})$ in the expression of the classical action given by Eq. (6) is the result of the fact that the propagator in Eq. (4) is given in imaginary time $t = -\imath\hbar\beta$ (the review of classical mechanics in imaginary time is given in Appendix A).

The form of the integral in Eq. (5) suggests that it can be analyzed within the stationary phase approximation. Within the stationary phase approximation, the value of the integral in Eq. (5) is dominated by stationary points of $S[\mathbf{x}(\tau)]$, i.e., by such trajectories $\mathbf{x}(\tau)$ that satisfy

$$\delta S[\mathbf{x}(\tau)] = 0. \tag{7}$$

The latter expression is the well-known variational principle of classical mechanics that is satisfied by classical trajectories $\mathbf{x}(\tau)$. There are two types of classical trajectories that satisfy the condition (7) on the inverted potential surface $-V(\mathbf{x})$.[8,21,28] One type of such trajectories is the trivial solution $\mathbf{x} \equiv \mathbf{x}_{\min}$, i.e., the trajectory that consists of one point and sits at the maximum of $-V(\mathbf{x})$, or, respectively, the minimum of $V(\mathbf{x})$. And the other type of trajectories is $\hbar\beta$-periodic classical trajectory, the *instanton*, that satisfies classical equations of motion

$$-\frac{\partial^2 \mathbf{x}}{\partial \tau^2} + \frac{\partial V(\mathbf{x})}{\partial \mathbf{x}} = 0. \tag{8}$$

Such classical periodic trajectories become possible since the barrier of the surface $V(\mathbf{x})$ becomes a potential well for the flipped potential $-V(\mathbf{x})$,[7] and, therefore, the possibility of bounded oscillations (instantons) appears. Yet, the degrees of freedom orthogonal to the instanton trajectory become unstable on the inverted potential surface $-V(\mathbf{x})$ and thus the instanton trajectory is an unstable periodic trajectory. The integral in Eq. (5), therefore, consists of two dominant contributions

$$Q = Q[\mathbf{x}_{\text{inst}}] + Q[\mathbf{x}_{\min}], \tag{9}$$

which are evaluated (in a path integral sense, by computing quantum fluctuations around the extremal classical trajectory) along the instanton trajectory and around the minimum $\mathbf{x} \equiv \mathbf{x}_{\min}$ of $V(\mathbf{x})$, respectively. The term $Q[\mathbf{x}_{\min}]$ is clearly just a partition function of reactants, i.e.,

$$Q[\mathbf{x}_{\min}] \equiv Q_r \tag{10}$$

and is pure real. The term $Q[\mathbf{x}_{\text{inst}}]$, which is due to the presence of a barrier, is pure imaginary as shown rigorously in Refs. 1, 2, and 21 and discussed at the beginning of the present section. The expression (3) for the reaction rate coefficient then becomes

$$k Q_r = \frac{2}{\hbar\beta} \text{Im} Q[\mathbf{x}_{\text{inst}}]. \tag{11}$$

To evaluate $Q[\mathbf{x}_{\text{inst}}]$ one defines a one-dimensional coordinate X along the classical instanton trajectory $\mathbf{x}_{\text{inst}}(\tau)$ that is a solution of Eq. (8) and an $(N-1)$-dimensional vector $\mathbf{Y}$ for the transverse displacements from the instanton trajectory. Assuming that transverse quantum fluctuations $\delta\mathbf{Y}$ are uncoupled from the longitudinal fluctuations δX, one can expand the action in Eq. (6) up to quadratic terms in $\delta\mathbf{Y}$ (Refs. 8, 28, 31, and 32)

$$S = \int_0^{\hbar\beta} \left[\frac{1}{2} \left(\frac{dX}{d\tau} \right)^2 + V(X(\tau)) \right] d\tau + \int_0^{\hbar\beta} \left[\frac{1}{2} \dot{\mathbf{Y}}^2 + \frac{1}{2} V''_{ij}(X(\tau)) Y_i Y_j \right] d\tau, \tag{12}$$

where $X(\tau) = X_{\text{inst}}(\tau) + \delta X(\tau)$ and $\mathbf{Y} = \delta\mathbf{Y}$. The second order derivative $V''_{ij}(X(\tau)) \equiv [\partial^2 V / \partial Y_i \partial Y_j]_{X(\tau),\mathbf{Y}=0}$ is taken at the point $\{X = X_{\text{inst}}(\tau), \mathbf{Y} = 0\}$ in the SI1 approximation discussed in Sec. III, or at the point $\{X = X(\tau), \mathbf{Y} = 0\}$ in the SI2 approximation discussed in Sec. IV, and thus parametrically depends on the value of $X_{\text{inst}}(\tau)$ or $X(\tau)$ (to cover both cases we use the notation $V''_{ij}(X(\tau))$). The direct evaluation of $V''_{ij}(X(\tau))$ is not a trivial procedure in multiple dimensions since for every point $X = X(\tau)$ on the instanton path (i.e., on the curve in many-dimensional space) one needs to make a transformation of the original coordinate system into an orthogonal coordinate system in which one of its axes is directed along the instanton path at $X = X(\tau)$. Fortunately, no direct evaluation of $[\partial^2 V / \partial Y_i \partial Y_j]$ is needed, the calculation of second order derivatives will be effectively performed by

evaluation of stability matrix along the instanton trajectory,[7,31] as discussed below.

Defining the instanton action with

$$S_0[X(\tau)] \equiv \int_0^{\hbar\beta} \left[\frac{1}{2} \left(\frac{dX}{d\tau} \right)^2 + V(X(\tau)) \right] d\tau, \quad (13)$$

the path integral expression (5) for $Q[\mathbf{x}_{\text{inst}}]$ then reads[13,28]

$$Q[\mathbf{x}_{\text{inst}}] = \int dX_0 \int_{X(0)=X_0}^{X(\hbar\beta)=X_0} D[X(\tau)] e^{-S_0[X(\tau)]/\hbar} \times \int d\mathbf{Y}_0 \int_{\mathbf{Y}(0)=\mathbf{Y}_0}^{\mathbf{Y}(\hbar\beta)=\mathbf{Y}_0} D[\mathbf{Y}(\tau)] e^{-\frac{1}{2\hbar}\int_0^{\hbar\beta}[\dot{\mathbf{Y}}^2 + V''_{ij}(X(\tau))Y_iY_j]d\tau}. \quad (14)$$

Integration over $\mathbf{Y}$ degrees of freedom in the path integral (14) can be performed exactly[28,32] and reads

$$\int d\mathbf{Y}_0 \int_{\mathbf{Y}(0)=\mathbf{Y}_0}^{\mathbf{Y}(\hbar\beta)=\mathbf{Y}_0} D[\mathbf{Y}(\tau)] e^{-\frac{1}{2\hbar}\int_0^{\hbar\beta}[\dot{\mathbf{Y}}^2 + V''_{ij}(X(\tau))Y_iY_j]d\tau} = \prod_{n=1}^{N-1} \frac{1}{2\sinh(\lambda_n/2)}, \quad (15)$$

where λ_n are stability parameters that correspond to the eigenvalues $e^{\pm\lambda_n}$ of the $2(N-1)$ dimensional stability matrix $\mathbf{R}_{2N-2}(\hbar\beta)$ evaluated along the instanton path. The stability matrix $\mathbf{R}_{2N-2}(\hbar\beta)$ is obtained from solution of the differential equation along the instanton trajectory[7]

$$\frac{d}{d\tau}\mathbf{R}_{2N-2}(\tau) + \mathbf{F}(\tau)\cdot\mathbf{R}_{2N-2}(\tau) = 0, \quad (16)$$

with the initial condition $\mathbf{R}_{2N-2}(0) = \mathbf{1}$. The matrix

$$\mathbf{F}(\tau) = \begin{pmatrix} \mathbf{0} & -\mathbf{1} \\ \dfrac{\partial^2 V}{\partial Y_i \partial Y_j} & \mathbf{0} \end{pmatrix}, \quad (17)$$

contains force constant parameters $V''_{ij}(\tau)$ from the path integral expression in Eq. (15), which change dynamically due to their parametric dependence on τ, i.e., on $X(\tau)$. The final value of $\mathbf{R}_{2N-2}$ at time $\tau = \hbar\beta$, i.e., after one full period of instanton trajectory, is the matrix whose eigenvalues are sought. If the coordinates $\mathbf{Y}$ were coordinates of $N-1$ independent one-dimensional harmonic oscillators with the corresponding frequencies ω_n (the force matrix $\mathbf{F}$ therefore would be constant), then the eigenvalues of $\mathbf{R}_{2N-2}(\hbar\beta)$ as found from Eqs.(16)–(17) would be $e^{\pm\omega_n\hbar\beta}$ with the corresponding stability parameters $\lambda_n = \omega_n\hbar\beta$. Substituting the latter stability parameters to Eq. (15) one obtains the product of partition functions of uncoupled harmonic oscillators $\prod_{n=1}^{N-1}[2\sinh(\omega_n\hbar\beta/2)]^{-1}$. Therefore, the stability parameters λ_n play the role of mean frequencies of transverse modes[7] multiplied by $\hbar\beta$, or, in other words, $\lambda_n/2\beta$ is approximately zero-point energy of the transverse mode Y_n.

In practical applications the stability parameters λ_n are obtained by solving for stability matrix in full N-dimensional space. For that, one appends the instanton degree of freedom X to the $(N-1)$-dimensional space $\{\mathbf{Y}\}$, making the combined $\{X, \mathbf{Y}\}$ space N-dimensional, and uses the property of invariance[7,31] of eigenvalues of stability matrix $\mathbf{R}_{2N}$ to the choice of orthogonal coordinate system, i.e., the eigenvalues of $\mathbf{R}_{2N}$ in the coordinate system $\{X, \mathbf{Y}\}$ and in the original N-dimensional configuration space $\{\mathbf{x}\}$ are the same. The two extra eigenvalues of stability matrix $\mathbf{R}_{2N}$ have zero stability parameter $\lambda = 0$ corresponding to the instanton degree of freedom $X(\tau)$ and manifests its invariance with respect to time shift.[10] A set of N stability parameters obtained from the stability matrix $\mathbf{R}_{2N}(\hbar\beta)$ is therefore $\{0, \lambda_1, \lambda_2, \ldots \lambda_{N-1}\}$, in which the nonzero λ_n's are used in expression (15). To obtain $\mathbf{R}_{2N}(\hbar\beta)$ one needs to propagate $\mathbf{R}_{2N}(\tau)$ according to

$$\frac{d}{d\tau}\mathbf{R}_{2N}(\tau) + \mathbf{F}_{2N}(\tau)\cdot\mathbf{R}_{2N}(\tau) = 0, \quad (18)$$

with the initial condition $\mathbf{R}_{2N}(0) = \mathbf{1}$ and

$$\mathbf{F}_{2N}(\tau) = \begin{pmatrix} \mathbf{0} & -\mathbf{1} \\ \dfrac{\partial^2 V}{\partial x_i \partial x_j} & \mathbf{0} \end{pmatrix}_{\text{inst}}, \quad (19)$$

where the Hessian matrix $\partial^2 V/\partial x_i \partial x_j$ is calculated on the instanton trajectory $\mathbf{x} = \mathbf{x}_{\text{inst}}(\tau)$.

Substituting Eq. (15) into Eq. (14) one obtains

$$Q[\mathbf{x}_{inst}] = \oint D[X(\tau)] e^{-S_0[X(\tau)]/\hbar} \prod_{n=1}^{N-1} \frac{1}{2\sinh\left(\frac{1}{2}\lambda_n[X(\tau)]\right)}. \quad (20)$$

The expression (20) is given in Ref. 28. The idea that we propose in the present paper is to take the integral over the instanton coordinate using its effective one-dimensional analog.

III. EFFECTIVE ONE-DIMENSIONAL BARRIER

Substituting Eq. (20) into Eq. (11) one obtains the expression for the reaction rate coefficient

$$kQ_r = \frac{1}{\hbar\beta}\left(2\text{Im} \oint D[X(\tau)] e^{-S_{\text{eff}}[X(\tau)]/\hbar} \right), \quad (21)$$

where we have defined the effective action

$$S_{\text{eff}} = \int_0^{\hbar\beta} \left[\frac{1}{2} \left(\frac{dX}{d\tau} \right)^2 + V(X(\tau)) \right] d\tau + \sigma[X(\tau)] \quad (22)$$

and

$$\sigma = \hbar \sum_{n=1}^{N-1} \ln\left(2\sinh\frac{\lambda_n}{2} \right). \quad (23)$$

As discussed in Sec. II, σ stands for zero-point energy contribution to the action from the transverse modes.

It has been noted in Refs. 2, 8, 21, and 24 that the imaginary part of a complex-valued partition function of a metastable system is exactly two times smaller than the pure imaginary partition function defined on its barrier, i.e.,

$$\text{Im}Q_{\text{inst}} = \frac{1}{2}\text{Im}Q_b. \quad (24)$$

The latter is because the integration over the longitudinal quantum fluctuations in the path integral of Eq. (21) after analytical continuation to imaginary plane is performed over

the half of the Gaussian peak in case of metastable one-dimensional potential well and over the full Gaussian peak for the "unbounded" one-dimensional barrier.[24,33] From the expressions (21) and (24) one can see that Eq. (21) is equivalent to the expression $f = (\hbar\beta)^{-1}\mathrm{Im}Q_b$ for the flux $f = kQ_r$ over some one-dimensional barrier[2] with the one-dimensional Euclidian barrier action given by Eq. (22). The equivalence of the original multidimensional metastability problem to the one-dimensional flux over the barrier problem simplifies our further analysis a lot, since the quantum mechanics of one-dimensional systems has been studied very well and the accurate semiclassical one-dimensional methods, such as WKB approximation,[34] are available. For instance, within the WKB approximation, the flux over some one-dimensional barrier $\widetilde{V}_b(s)$ at low temperatures reads[2]

$$f = \frac{1}{2\pi\hbar}\int_{-\infty}^{\widetilde{V}_0} e^{-\beta\widetilde{E}}e^{-\widetilde{W}(\widetilde{E})/\hbar}d\widetilde{E}, \tag{25}$$

where $\widetilde{W}(\widetilde{E})$ is a shortened action $\widetilde{W}(\widetilde{E}) = \oint\sqrt{2(\widetilde{V}(s)-\widetilde{E})}ds$ and $\widetilde{V}_0$ is the height of the one-dimensional barrier $\widetilde{V}_b(s)$. Our goal is to identify the effective barrier $\widetilde{V}_b(s)$ that corresponds to the full action S_{eff} in Eq. (22). Clearly we will not be able to identify the functional form of $\widetilde{V}_b(s)$, what we need instead is its parameters such as shortened action, barrier height, curvature at the barrier, etc. Everywhere in this paper we use tilde hat to indicate (classical) parameters related to the effective one-dimensional barrier $\widetilde{V}_b(s)$, while the parameters without tilde hats are related to the original N-dimensional problem.

If we employ Gutzwiller approximation[28,31] that the stability parameters λ_n depend only on the classical instanton path $X_{\mathrm{inst}}(\tau)$ then λ_n are constants in the path integral (21). Since in most cases for every temperature β there exists only one classical periodic trajectory of period $\tau_\beta \equiv \hbar\beta$, then the stability parameters λ_n, evaluated along this classical trajectory, are functions of τ_β. In other words, in Gutzwiller approximation we have $\lambda_n(X(\tau)) = \lambda_n(X_{\mathrm{inst}}(\tau)) = \lambda_n(\tau_\beta)$. From Eq. (22) one can then obtain the classical action $\widetilde{S}$ (in fact, S_{eff} in Eq. (22) is already classical) that corresponds to one full period of τ_β-periodic classical trajectory in the inverted one dimensional barrier $\widetilde{V}_b$

$$\widetilde{S} = \int_0^{\tau_\beta}\left[\frac{1}{2}\left(\frac{dX}{d\tau}\right)^2 + V(X(\tau))\right]d\tau + \sigma(\tau_\beta). \tag{26}$$

Varying $\widetilde{S}$ with respect to X at constant τ_β one obtains classical equation of motion on the inverted (yet, unknown) barrier $\widetilde{V}_b(X)$ to be the same as the classical equation of motion for the instanton $X_{\mathrm{inst}}(\tau)$ on the original N-dimensional surface [Eq. (8)], i.e., the potential barrier $\widetilde{V}_b(X)$ originates from the set of one-dimensional instanton potentials $V(\mathbf{x}_{\mathrm{inst}})$ at different β's. Suppose a classical unstable periodic trajectory, i.e., the instanton, of period τ_β is found on the inverted N-dimensional PES $-V(\mathbf{x})$. Then this classical periodic trajectory corresponds to the energy $E_0(\tau_\beta)$ and has a full action S_0 after one period of oscillation τ_β. Clearly $E_0 = \partial S_0(\tau_\beta)/\partial\tau_\beta$ as shown in Appendix B. Using these definitions we have

$$\widetilde{S}(\tau_\beta) = S_0(\tau_\beta) + \sigma(\tau_\beta), \tag{27}$$

and the energy of the classical periodic trajectory of period τ_β that corresponds to the full classical action $\widetilde{S}(\tau_\beta)$ (on the inverted potential $-\widetilde{V}_b(s)$) is therefore

$$\begin{aligned}\widetilde{E}(\tau_\beta) &= \frac{\partial\widetilde{S}(\tau_\beta)}{\partial\tau_\beta}\\ &= E_0(\tau_\beta) + \frac{d\sigma(\tau_\beta)}{d\tau_\beta}.\end{aligned} \tag{28}$$

Interestingly, if the stability parameters λ_n corresponded to uncoupled harmonic oscillators $\lambda_n = \hbar\omega_n\beta$, as discussed in Sec. II, then $\sigma = \hbar\sum_n \ln[2\sinh(\hbar\omega_n\beta/2)] \approx \sum_n \hbar\omega_n\tau_\beta/2$ and therefore $d\sigma/d\tau_\beta = \sum_n \hbar\omega_n/2$ is the total zero-point energy of all transverse modes. At this point we note that because of the linear dependence of $\hbar\omega_n\tau_\beta/2$ on τ_β for a system of uncoupled harmonic oscillators, the simple ratio σ/τ_β will also produce the same result as $d\sigma/d\tau_\beta$. While in the limit of uncoupled transverse harmonic modes both σ/τ_β and $d\sigma/d\tau_\beta$ give similar results, it is generally not true in case of nonseparable systems.

Given with the energy $\widetilde{E}$ of the trajectory and its full action $\widetilde{S}$ one can find the corresponding shortened action $\widetilde{W}$, see Appendix A

$$\begin{aligned}\widetilde{W} &= \widetilde{S} - \tau_\beta\widetilde{E}\\ &= (S_0 - \tau_\beta E_0) + \sigma(\tau_\beta) - \tau_\beta\frac{d\sigma(\tau_\beta)}{d\tau_\beta}\\ &= W_0(\tau_\beta) + \sigma(\tau_\beta) - \tau_\beta\frac{d\sigma(\tau_\beta)}{d\tau_\beta},\end{aligned} \tag{29}$$

where $W_0(\tau_\beta) = S_0(\tau_\beta) - \tau_\beta E_0(\tau_\beta)$ is the instanton's shortened action on the inverted original multidimensional PES. The expression for $\widetilde{W}$ can be rewritten in the equivalent form

$$\widetilde{W}(\tau_\beta) = W_0(\tau_\beta) - \tau_\beta^2\frac{d}{d\tau_\beta}\left(\frac{\sigma(\tau_\beta)}{\tau_\beta}\right). \tag{30}$$

Here we comment on expression (30). It is well known,[27,28,32] that there is an upper limit of temperatures that allows an existence of instanton trajectories. Indeed, a period τ_β of instanton trajectory, i.e., of classical periodic orbit on the inverted potential surface $-V(\mathbf{x})$, is directly related to the inverse temperature β: $\tau_\beta = \hbar\beta$. Yet, from mechanical perspective, a period of oscillation of classical trajectory on the surface $-V(\mathbf{x})$ cannot be smaller than $2\pi/\omega_b$, where ω_b is the harmonic frequency of the unstable mode at the barrier top of PES $V(\mathbf{x})$. Therefore as temperature increases up to $T_c = \omega_b\hbar/(2\pi\kappa_B)$, instanton trajectories shrink down to the point located at the barrier top, i.e., at the saddle point of the N-dimensional PES $V(\mathbf{x})$. At temperatures $T > T_c$, an instanton trajectory consists of a single point that sits at the barrier top of $V(\mathbf{x})$. The shrinking of instanton trajectories to the barrier top at higher temperatures has simple physics. Instanton trajectory stands for the most probable tunneling path at a given temperature. The lower the temperature is, the longer is the instanton trajectory and the larger are the tunneling effects. As the temperature increases, the tunneling effects become less and less important and the instanton trajectory shrinks correspondingly.

It is interesting now to take a look at how $\widetilde{W}(\tau_\beta)$ behaves as temperature increases to its critical value T_c. Normally the frequencies of transverse degrees of freedom decrease along the minimum energy path (MEP) on PES from reactants well toward the barrier top and therefore their combined zero-point energy decreases as well. As temperature increases, instanton trajectories tend to localize closer to the barrier top and therefore the corresponding zero-point energy of transverse fluctuations tend to decrease as well, implying positive derivative $d(\sigma(\tau_\beta)/\tau_\beta)/d\tau_\beta$ in Eq. (30). The latter makes $\widetilde{W}(\tau_\beta)$ to be always lower than $W_0(\tau_\beta)$. At the critical temperature, instanton trajectory shrinks to the point resulting in zero value of W_0, which therefore implies *negative* value of $\widetilde{W}$. The negative value of $\widetilde{W}$, yet, should not lead to confusion: in the case of harmonic barrier with the barrier top at $E = V_0$, its shortened action that appears in the expression of exact transmission coefficient $D = 1/(1 + \exp(-W(E)))$ reads $W(E) = (2\pi/\omega)(V_0 - E)$ and is valid at all energies.[1,34] Negative $\widetilde{W}$ at $T = T_c$ means that the corresponding energy $\widetilde{E}$ is already above the barrier top $\widetilde{V}_0$. To find the value of $\widetilde{V}_0$ we therefore need to find such energy $\widetilde{E} = \widetilde{E}(\tau_\beta^*)$ (or, respectively, to find such τ_β^*) that corresponds to $\widetilde{W}(\tau_\beta^*) = 0$. Thus, we have

$$\widetilde{V}_0 = \widetilde{E}(\tau_\beta^*), \tag{31}$$

where τ_β^* is such that

$$\widetilde{W}(\tau_\beta^*) = 0. \tag{32}$$

The latter defines the critical temperature that corresponds to the vanishing of classical periodic trajectories on the effective inverted barrier $-\widetilde{V}_b(s)$

$$\widetilde{T}_c = \frac{\hbar}{\tau_\beta^* \kappa_B}. \tag{33}$$

From Eq. (33) we therefore can find the curvature of the effective one-dimensional barrier $\widetilde{V}_b(s)$ at its top

$$\widetilde{\omega}_b = \frac{2\pi}{\tau_\beta^*}, \tag{34}$$

where $\widetilde{\omega}_b$ is the harmonic frequency at the top of the barrier $\widetilde{V}_b(s) \approx -\widetilde{\omega}_b^2 s^2/2$.

IV. EXPRESSIONS FOR RATE COEFFICIENTS

We now have all parameters $\widetilde{S}(\beta)$, $\widetilde{W}(\beta)$, $\widetilde{E}(\beta)$, $\widetilde{V}_0$, and $\widetilde{T}_c$ which are necessary for semiclassical description of the flux over the effective one-dimensional barrier $\widetilde{V}(s)$. The semiclassical expression for the flux over one-dimensional barrier at different temperatures has been rigorously derived, for instance, in Ref. 2 and was shown there to be very accurate. The latter derivations are reviewed in Appendix C. Using the results for the flux over one dimensional barrier either from Ref. 2 or from Appendix C, we immediately obtain the expressions for the rate coefficient k of a multidimensional reaction.

For temperatures $T < \widetilde{T}_c$ the reaction rate coefficient is given by

$$\begin{aligned} kQ_r &= \sqrt{\frac{-\widetilde{E}'(\beta)}{2\pi\hbar^2}} e^{-\widetilde{S}(\beta)/\hbar} \mathrm{erf}\left[\frac{\widetilde{V}_0 - \widetilde{E}(\beta)}{\sqrt{-\widetilde{E}'(\beta)}}\right] \\ &= \sqrt{\frac{-E_0'(\beta) - \sigma''(\beta)}{2\pi\hbar^2}} e^{-S_0(\beta)/\hbar} \prod_{n=1}^{N-1} \frac{1}{2\sinh\left(\frac{1}{2}\lambda_n(\beta)\right)} \\ &\quad \times \mathrm{erf}\left[\frac{\widetilde{V}_0 - E_0(\beta) - \sigma'(\beta)}{\sqrt{-E_0'(\beta) - \sigma''(\beta)}}\right], \end{aligned} \tag{35}$$

where $E_0(\beta)$,$S_0(\beta)$ are the energy and the Euclidian action, respectively, of the classical $\hbar\beta$-periodic instanton on the inverted multidimensional PES, and $\beta = 1/\kappa_B T$ is the inverse temperature. The parameter $\sigma(\beta)$ is zero-point energy contribution of $N-1$ transverse fluctuations around the instanton path and is given by Eq. (23). Dash sign indicates the derivative $d/d\beta$. The error-function $\mathrm{erf}(x)$ is defined in Appendix B.

For temperatures $T \geq \widetilde{T}_c$ the reaction rate coefficient is given by

$$kQ_r = \mathrm{Corr}\,(\Delta)\, \frac{1}{2\hbar\widetilde{\beta}_c \sin(\pi\beta/\widetilde{\beta}_c)} e^{-\beta\widetilde{V}_0}, \tag{36}$$

where $\widetilde{\beta}_c \equiv 1/\kappa_B\widetilde{T}_c = 2\pi/\hbar\widetilde{\omega}_b$ and

$$\mathrm{Corr}(\Delta) = \Delta\sqrt{2\pi}\,\mathrm{erf}(-\Delta)e^{\Delta^2/2}, \tag{37}$$

with

$$\Delta = \frac{\beta}{2}\left(\left(\frac{\widetilde{\beta}_c}{\beta}\right)^2 - 1\right)\sqrt{-E_0'(\widetilde{\beta}_c) - \sigma''(\widetilde{\beta}_c)}. \tag{38}$$

In the high-temperature limit the correction factor $\mathrm{Corr}(\Delta)$ becomes equal to 1 and expression (36) coincides with the exact expression for a quantum flux over the parabolic barrier. As it was shown in Ref. 2, see Appendix C, expressions (35) and (36) coincide in the vicinity of $\widetilde{T}_c$.

Equation (35) looks very similar to Eq. (2.34) of Ref. 7, derived with quantum transition state theory approach, yet with several differences. We discuss them in Sec. V as well as indicate a connection of the present semiclassical approach to other reaction rate theories.

V. RELATION TO OTHER RATE THEORIES

Several semiclassical rate theories have been developed in the past to account for multidimensional tunneling. In this section we show how they are related to the semiclassical instanton approximation discussed in the present paper.

A. Classical transition state theory

The classical transition state theory rate coefficient can be obtained from Eq. (36) in the limit of high temperature. Indeed, at high temperatures (i.e., small β's) we have $\mathrm{Corr}(\Delta) = 1$ as shown in Appendix C. Thus Eq. (36) reads

$$kQ_r = \frac{1}{2\pi\hbar\beta} e^{-\beta\widetilde{V}_0}. \tag{39}$$

The height of the effective potential barrier $\widetilde{V}_0$ already contains quantized transverse degrees of freedom as follows from Eq. (31)

$$\widetilde{V}_0 \equiv E_0(\tau_\beta^*) + \sigma'(\tau_\beta^*). \tag{40}$$

As discussed in Sec. IV, the period τ_β^* corresponds to the instanton trajectory that is almost shrinked to the point located at the barrier top of PES. Therefore $E_0(\tau_\beta^*) \approx V_0$, where V_0 is the saddle point of PES, i.e., the top of the barrier along the minimum energy path on PES. As we discussed in Sec. III, derivative $\sigma'(\tau_\beta^*)$ is approximately the combined zero-point energy along the instanton trajectory. Since the instanton trajectory that corresponds to τ_β^* almost coincides with the barrier top then its transverse frequencies are exactly the transverse frequencies $\omega_n^\#$ at the saddle point of PES. Therefore $\sigma'(\tau_\beta^*) \approx \sum_n \hbar\omega_n^\#/2$. Expression (39) thus becomes

$$k = \frac{1}{2\pi\hbar\beta}\frac{1}{Q_r}\exp\left(-\beta V_0 - \beta\sum_{n=1}^{N-1}\frac{\hbar\omega_n^\#}{2}\right)$$
$$= \frac{1}{2\pi\hbar\beta}\frac{Q^\#}{Q_r}e^{-\beta V_0}, \tag{41}$$

where the partition function of transition state $Q^\#$ is

$$Q^\# = \prod_{n=1}^{N-1} Q_n^\# = \prod_{n=1}^{N-1}\frac{1}{2\sinh\left(\frac{\hbar\omega_n^\#\beta}{2}\right)} \approx \prod_{n=1}^{N-1} e^{-\beta\hbar\omega_n^\#/2}. \tag{42}$$

Expression (41) is the reaction rate coefficient from the classical transition state approach.

B. Quantum transition state theory

There are several versions of quantum transition state theory in the literature.[6,7,35–39] We consider the semiclassical version of quantum transition state theory developed by Miller in Ref. 7 for comparison. The low-temperature rate coefficient expression given by Eq. (2.34) in the latter work,

$$kQ_r = \sqrt{\frac{-E_0'(\beta)}{2\pi\hbar^2}}e^{-S_0(\beta)/\hbar}\prod_{n=1}^{N-1}\frac{1}{2\sinh\left(\frac{1}{2}\lambda_n(\beta)\right)}, \tag{43}$$

is almost the same as the instanton expression (35) of the present paper. The difference is only in the erf function to account for truncation of the integral over energy at the barrier top and in the presence of zero-point energy $\sigma'(\beta)$ in the pre-exponential factor. The latter is due to the fact that in the original theory by Miller, the total microcanonical energy of reacting system that corresponded to the instanton of period $\hbar\beta$ was the energy of instanton, i.e., $E = E_0(\beta)$, while in the present semiclassical theory, the total microcanonical energy of reacting system is $E = \widetilde{E}(\beta) = E_0(\beta) + \sigma'(\beta)$, i.e., the combined energy of instanton *and* zero-point energy of transverse fluctuations. This difference was the reason for the observed poor agreement[18] of the original instanton theory[7] with the exact quantum results for microcanonical reaction probability and therefore required a correction.[18]

To illustrate the above argument we plot the cumulative microcanonical reaction probability $N(E)$ and compare it to the result of the paper,[18] (see Fig. 1). In Secs. III and IV

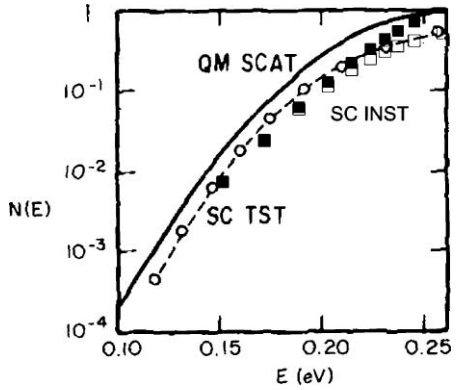

FIG. 1. Microcanonical reaction probability $N(E)$ for the collinear reaction $H + H_2 \rightarrow H_2 + H$ on the Porter–Karplus PES II. Energy E stands for the total energy E_{total} reduced by zero-point energy of H–H vibration of H_2 molecule, $E = E_{\text{total}} - \hbar\omega_{H_2}/2$. "QM SCAT" (solid line) stands for exact quantum result from scattering theory, "SC TST" (open circles) is the corrected semiclassical transition state theory result of Ref. 18 and "SC INST" (squares) is the semiclassical instanton result of the present paper (SI1 instanton theory) with $E_{\text{total}} \equiv \widetilde{E}$. Results are shown for two forms of transmission coefficients: $N(\widetilde{E}) = \exp(-\widetilde{W}(\widetilde{E}))$ (solid squares); $N(\widetilde{E}) = 1/(1 + \exp[\widetilde{W}(\widetilde{E})])$ (open squares). The plot of Ref. 18 is reprinted with permission from S. Chapman, B. C. Garrett, and W. H. Miller, J. Chem. Phys. **63**, 2710 (1975). Copyright 1975, American Institute of Physics.

we have shown that the original N-dimensional problem is equivalent to the effective one-dimensional barrier penetration problem with the WKB action $\widetilde{W}$ corresponding to an incident particle of energy $\widetilde{E}$ (they depend on each other parametrically as $\widetilde{E}(\beta)$ with $\widetilde{W}(\beta)$). We can now write down the corresponding WKB transmission coefficient $N(\widetilde{E}) = 1/(1 + \exp(\widetilde{W}(\widetilde{E})))$. In fact, in the one-dimensional instanton approximation,[2] used to derive Eq. (35), the original noncorrected transmission coefficient[34] $N(\widetilde{E}) = \exp(-\widetilde{W}(\widetilde{E}))$ is used. We compare both expressions in Fig. 1. One observes agreement within a factor of 2 with the exact quantum results. It should be noted, that the semiclassical results of Ref. 18, plotted in Fig. 1, are the corrected results.

C. Zero-, small-, and large-curvature tunneling paths

Several quantum tunneling paths have been suggested in the past to incorporate quantum tunneling effects based on physical intuition.[5,6] They are zero-curvature path, which coincides with the MEP on PES for potential surfaces of low curvature; small-curvature path, which is taken on the concave side of the minimum energy path for PES of medium curvature; and large-curvature path, which is a straight-line path and is applied for PES of very high curvature of MEP. All of the listed paths are the particular cases of instanton paths, as one can see from dynamics of a classical particle on the inverted potential surface. Indeed, for PES $V(\mathbf{x})$ of zero MEP curvature the periodic classical path on the inverted potential $-V(\mathbf{x})$ is the one that lies exactly on the MEP. For the inverted potential $-V(\mathbf{x})$ the minimum energy path becomes the "maximum" energy path, and therefore the periodic classical trajectory should lie right along this path not to "fall off" the surface $-V(\mathbf{x})$. If MEP contains some curvature, than the classical periodic trajectory on surface $-V(\mathbf{x})$ should lie on

the concave side of MEP to compensate for the additional centrifugal force resulting from the path curvature. The latter is exactly the negative centrifugal effect employed in the small curvature approximation. For large curvatures of MEP the instanton path is more like a straight line cut [see Fig. 2(d)] justifying the large curvature approximation.[40]

VI. IMPROVED SEMICLASSICAL INSTANTON APPROXIMATION (SI2)

The instanton approximation can be further improved if the Gutzwiller approximation is not used. Gutzwiller approximation assumed the dependence of stability parameters λ_n only on classical trajectories, the latter effectively introduced additional energy shift $\sigma'(\beta)$ to the instanton energy without perturbing instanton trajectory itself. If one now assumes that the stability parameters λ_n depend on quantum trajectory $X(\tau)$ in the path integral (20) instead of being constant for given β, then the effective classical trajectory of instanton changes as well and its equation of motion reads[28]

$$\frac{\delta S_{\text{eff}}}{\delta X} = -\frac{\partial^2 X}{\partial \tau^2} + \frac{\partial V(X)}{\partial X} + \frac{1}{2}\sum_n \frac{\delta \lambda_n}{\delta X} \coth\left(\frac{1}{2}\lambda_n\right) = 0. \tag{44}$$

The last term introduces effective renormalization of instanton's potential[32]

$$V(X) \to V(X) + \sum_n \hbar\omega_n(X(\tau))/2, \tag{45}$$

where $\omega_n(X(\tau))$ are harmonic frequencies of transverse degrees of freedom along the instanton trajectory and have a clear physical meaning: since along the classical instanton path the curvature of PES for orthogonal degrees of freedom is not constant, then the zero-point energy of transverse degrees of freedom along the instanton path is not constant as well (for instance, in the beginning of instanton trajectory, at time $\tau = 0$ the transverse harmonic frequencies are those of reactants vibrational frequencies, while at time $\tau = \hbar\beta/4$ the transverse harmonic frequencies are closer to those of transition state). This change of zero-point energy of transverse degrees of freedom along the instanton path influences the effective potential energy of instanton correcting it by $\sum_n \hbar\omega_n(X)/2$. (In the Gutzwiller's approximation the latter correction was constant, independent of X). In this sense the instanton trajectory is not classical any more, but instead semiclassical. It should be noted that to find the corrected instanton path one cannot find the classical instanton path on the inverted PES and then correct its potential with zero-point energies $\sim \sum_n \hbar\omega_n(X)/2$. Instead, the classical trajectory $X_{cl}(\tau)$ that minimizes the action

$$\widetilde{S} = \int_0^{\hbar\beta} \left[\frac{1}{2}\left(\frac{dX}{d\tau}\right)^2 + V(X(\tau))\right] d\tau + \sigma[X(\tau)], \tag{46}$$

needs to be found. The numerical method that we use to search for the classical instanton trajectories is presented in Sec. VII and is capable to directly minimize either of actions $\widetilde{S}$ of Eq. (26) or $\widetilde{S}$ of Eq. (46), although minimization of the $\widetilde{S}$ in Eq. (46) requires more computations and is less stable.

Once the classical action $\widetilde{S}(\tau_\beta)$ is found for a given $\tau_\beta \equiv \hbar\beta$, then by analogy to the discussion of Sec. III we find its corresponding one-dimensional classical parameters

$$\widetilde{E}(\tau_\beta) = \frac{\partial \widetilde{S}(\tau_\beta)}{\partial \tau_\beta},$$

$$\widetilde{W}(\tau_\beta) = \widetilde{S}(\tau_\beta) - \tau_\beta \frac{\partial \widetilde{S}(\tau_\beta)}{\partial \tau_\beta},$$

$$\widetilde{V}_0 = \widetilde{E}(\tau_\beta^*), \tag{47}$$

where τ_β^* is such that $\widetilde{W}(\tau_\beta^*) = 0$. And the expressions for the reaction rate coefficient are

$$kQ_r = \sqrt{\frac{-\widetilde{E}'(\beta)}{2\pi\hbar^2}} e^{-\widetilde{S}(\beta)/\hbar} \text{erf}\left[\frac{\widetilde{V}_0 - \widetilde{E}(\beta)}{\sqrt{-\widetilde{E}'(\beta)}}\right], \tag{48}$$

for temperatures below the critical temperature $T < \widetilde{T}_c$; and

$$kQ_r = \Delta\sqrt{2\pi}\,\text{erf}(-\Delta) e^{\Delta^2/2} \frac{1}{2\hbar\widetilde{\beta}_c \sin(\pi\beta/\widetilde{\beta}_c)} e^{-\beta\widetilde{V}_0} \tag{49}$$

with

$$\Delta = \frac{\beta}{2}\left(\left(\frac{\widetilde{\beta}_c}{\beta}\right)^2 - 1\right)\sqrt{-\widetilde{E}'(\widetilde{\beta}_c)}. \tag{50}$$

for temperatures above the critical temperature $T \geq \widetilde{T}_c$, where $\widetilde{\beta}_c \equiv 1/\kappa_B \widetilde{T}_c = \tau_\beta^*/\hbar$.

The results of both instanton approximations are compared in Sec. VII.

VII. PRACTICAL APPLICATION OF SEMICLASSICAL INSTANTON THEORY IN MULTIPLE DIMENSIONS

Although the analytical expressions for reaction rate coefficients (35)–(38) or (48)–(50) are simple, the search of the classical periodic trajectory on arbitrary potential energy surfaces is not a trivial task. Indeed, a classical instanton trajectory is unstable in a sense that any arbitrary small deviation from the trajectory will result in exponential divergence away from it with the Lyapunov exponent given by the largest of stability parameters λ_n. Instanton trajectories in this sense are similar to the unstable periodic orbits of chaotic billiards.[41] The search of instanton trajectories by looking for their initial conditions is therefore an extremely ill-posed numerical problem.[42]

There exist several methods in literature for the search of instanton trajectories.[10,15–17] In this section we propose another algorithm which turned out to be sufficiently stable, intuitive, and simple. The method employs decomposition of instanton trajectory in Fourier series over the Matsubara frequencies $\nu_j = 2\pi j/\hbar\beta$.[27] Indeed, since an instanton trajectory is $\hbar\beta$-periodic, then every degree of freedom $\mathbf{x}$ of our N-dimensional system is $\hbar\beta$-periodic and we can decompose them in Fourier series

$$\mathbf{x}(\tau) = \sum_{j=0}^{\infty} \mathbf{C}_j \cos\left(\frac{2\pi j}{\hbar\beta}\tau\right). \tag{51}$$

The resulting path $\mathbf{x}(\tau)$ is clearly a one-dimensional curve in the N-dimensional space parameterized by parameter τ.

Taking path-integrals by Fourier analysis is a well-known procedure.[29,43] Yet, while quantum paths are nonsmooth and thus require a large number of Fourier coefficients, the classical instanton paths are smooth and therefore require a small number of Fourier coefficients. For instance, to find a classical instanton trajectory at temperatures close to the critical, T_c, as few as two Fourier coefficients C_{n0} and C_{n1} are required for each degree of freedom $x_n(\tau)$, since near the barrier top the oscillations of instanton are almost perfectly harmonic.

We substitute Eq. (51) into Eq. (6) and reduce the problem of finding classical instanton trajectory to the optimization problem

$$\delta S(\mathbf{C}_j) = 0, \tag{52}$$

or equivalently to the system of $N \times J$ equations

$$\frac{2\pi^2 j^2}{\hbar\beta} C_{nj} + \int_0^{\hbar\beta} \frac{dV(\mathbf{x}(\mathbf{C}))}{dx_n} \cos\left(\frac{2\pi j}{\hbar\beta}\tau\right) d\tau = 0, \tag{53}$$

where $n = 1, 2, \ldots, N$ numerates system's degrees of freedom and $j = 1, 2, .., J$ numerates the set of Fourier coefficients required for each degree of freedom. Solution of Eq. (52) can be performed by various methods such as Newton–Raphson method or the method of steepest descents.

We use Newton–Raphson method as the primary method to solve for unknown Fourier coefficients. We proceeded as follows.

1. As we know, instanton trajectories at high temperatures collapse to the saddle point of PES. By setting some arbitrary high temperature value for β and knowing an approximate region of saddle point location (in fact for some simple surfaces we may know the location of the saddle point exactly) we run the Newton–Raphson method with only a single zero-order Fourier coefficient C_{n0} in each degree of freedom, i.e., $x_n = C_{n0}$. The Newton–Raphson method converges to the point $\{C_{10}, C_{20}, \ldots, C_{N0}\}$, which is the saddle point of PES.

2. We then lower the temperature and include another Fourier coefficient, C_{n1}, i.e., now we represent system's degrees of freedom in the form $x_n = C_{n0} + C_{n1}\cos(2\pi\tau/\hbar\beta)$. We set initial values of C_{n1} to be some random small numbers in the vicinity of zero and take previously found values of C_{n0} as initial values for C_{n0}. If the taken temperature is lower than the critical temperature T_c, then the numerical algorithm will converge to nonzero values of C_{n1} indicating the birth of classical instantons.

3. To improve the classical instanton trajectory at a given temperature or to find the instanton trajectory at lower temperatures one includes more and more Fourier coefficients C_{nj} taking the values of the Fourier coefficients found at the previous step as initial values in the Newton–Raphson method. The initial values of newly introduced Fourier coefficients can be taken as zero. The procedure of adding more Fourier coefficients repeats until their converged values become smaller than some predefined precision. In our case we truncated Fourier expansion when the absolute values of coefficients C_{nj} and $C_{n,j+1}$ became smaller than $10^{-5}C_{n1}$.

Following the above procedure we performed numerical search of classical periodic trajectories on potential energy surfaces of seven different collinear reactions. We started with three Fourier coefficients to search for instantons for temperatures near the critical (in fact, the critical temperature was determined by the fact of appearance of instantons). Then by the ladder algorithm described above, introducing 2–3 new Fourier coefficients at a time, we "pulled" the numerical search algorithm down to the temperatures of 150 K, recording the converged instanton trajectories at each temperature as well as their energies $E_0(\beta)$, classical actions $W_0(\beta)$, $S_0(\beta)$, and stability parameters λ_n along them. In the deep tunneling regime, at temperatures 150 K, the maximum number J of Fourier coefficients in each degree of freedom that are necessary to obtain the instanton trajectory with the precision $|C_{nJ} < 10^{-5}C_{n1}|$ was found to be no more than 16.

If the instanton trajectory $\mathbf{x}(\tau) = \sum_{j=0}^{J} \mathbf{C}_j \cos(2\pi j/\hbar\beta\tau)$ is found, the calculation of stability parameters λ_n along this trajectory is trivial. The force matrix (19) is calculated at any time τ by evaluating the derivative $\partial^2 V(\mathbf{x})/\partial x_i x_j$ at the point $\mathbf{x} = \mathbf{x}(\tau)$. The Runge–Kutta algorithm is then used to solve Eq. (18) for stability matrix $\mathbf{R}_{2N}(\hbar\beta)$, eigenvalues of which provide stability parameters λ_n as discussed in Sec. II.

To evaluate derivatives over β such as $E_0'(\beta)$ or $\sigma''(\beta)$ the well-known finite difference schemes such as $E_0'(\beta) = [E_0(\beta + \Delta\beta) - E_0(\beta - \Delta\beta)]/2\Delta\beta$ can be used, or interpolation of data points with a smooth function can be employed. The latter is preferable for plots of small curvature to reduce the error.

We also test the slightly improved instanton approximation of Sec. IV. To find instanton trajectories of the latter approximation one needs to solve optimization problem of the form $\delta(S(\mathbf{C}_j) + \sigma(\mathbf{C}_j)) = 0$. The latter task is computationally more demanding since each step of Newton–Raphson method requires computation of stability parameters $\lambda_n(\mathbf{C}_j)$. To do this, we first find the classical instanton trajectory that corresponds to $\delta S(\mathbf{C}_j) = 0$ using Newton–Raphson method described above and then take these values of Fourier coefficients $\mathbf{C}_j$ as initial values to "fine-tune" the new optimization problem $\delta(S(\mathbf{C}_j) + \sigma(\mathbf{C}_j)) = 0$ using the steepest descent method.

VIII. NUMERICAL RESULTS

We have tested the revisited semiclassical instanton approximations SI1 and SI2, i.e., Eqs. (35)–(38) and Eqs. (48)–(50) respectively, on seven collinear symmetric and asymmetric atom transfer reactions and calculated their quantum canonical reaction rate coefficients in the wide range of temperatures from 150 to 1500 K. Although in Secs. II and III we used the term "potential well" when referring to reactant states, it is clear that the same arguments are applicable to unbounded atom–diatom systems, in this case the minimum of potential well is located at infinity. The partition function of reactants per unit volume were calculated from the expression

$$Q_r = \sqrt{\frac{\mu_{\mathrm{A,BC}}}{2\pi\hbar^2\beta}} Q_v, \tag{54}$$

where $\mu_{A,BC}$ is the reduced mass of atom–diatom pair and

$$Q_v = \frac{1}{2\sinh\left(\hbar\omega_{BC}\beta/2\right)} \tag{55}$$

is the vibrational partition function of diatomic molecule. The latter does not incorporate anaharmonicity effects to be on the same footage[8,32] with the semiclassical instanton approximation which considers only quadratic fluctuations around the instanton trajectory.

A. $H + H_2 \rightarrow H_2 + H$

To calculate the rate constants of the atom transfer collinear reaction $H + H_2 \rightarrow H_2 + H$, we picked the well-studied Porter–Karplus potential energy surface (number 2) of Ref. 44. The exact quantum mechanical canonical rate constants for this surface are given in Ref. 45. The semiclassical rate coefficients were calculated from Eqs. (35)–(36) of SI1 version of instanton theory described in Secs. II–V and Eqs. (48)–(49) of SI2 version instanton theory, which is described in Sec. VI. Some classical instanton trajectories on inverted PES (i.e., instanton trajectories of SI1 approximation) that correspond to different temperatures are shown in Fig. 2(b). The difference between instanton trajectories of SI1 and SI2 approximation is shown in Fig. 3(a). The reason for the difference is in the additional zero-point energy potential of transverse degrees of freedom in SI2 approximation.

The dependence of the effective one-dimensional parameters $\widetilde{W}$ and $\widetilde{E}$ on inverse temperature β, i.e., on the period of the corresponding $\hbar\beta$-periodic classical trajectories, is shown in Fig. 4, and was calculated from Eqs. (28)–(29) and (47) of SI1 and SI2 approximation, respectively. From the plot of $\widetilde{W}(\beta)$ one easily finds the critical temperatures $\widetilde{T}_c = 1/\kappa_B\widetilde{\beta}_c$ that correspond to $\widetilde{W}(\widetilde{\beta}_c) = 0$, pointed in Fig. 4 with arrows.

The canonical rate constants calculated within SI1 and SI2 approximations are shown in Fig. 5 and are compared there with the exact quantum rate coefficients. SI1 instanton approximation observes agreement within a factor of 2 with exact results, while SI2 approximation is accurate to within a factor of 1.5. Both approximations show improved agreement at higher temperatures.

B. $Cl + H_2 \rightarrow ClH + H$ and $Cl + D_2 \rightarrow ClD + D$

Collinear reactions $Cl + H_2 \rightarrow ClH + H$ and $Cl + D_2 \rightarrow ClD + D$ are good examples of highly

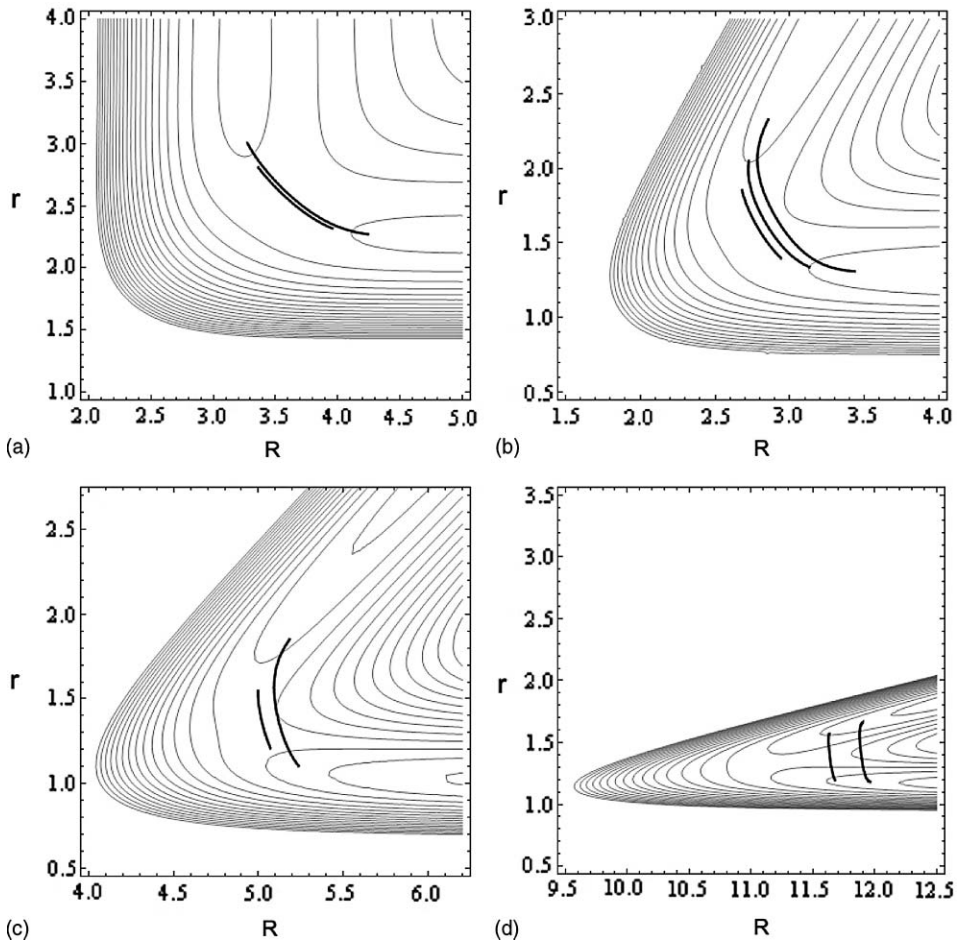

FIG. 2. Classical periodic trajectories on PES. These trajectories are the instanton trajectories of SI1 instanton theory. Insets (a)–(d) show instantons for collinear reactions at different temperatures (longer instanton trajectories correspond to lower temperatures): (a) $D + BrH \rightarrow DBr + H$ at 200 and 150 K; (b) $H + H_2 \rightarrow H_2 + H$ at 400, 300, and 200 K; (c) $Cl + H_2 \rightarrow ClH + H$ at 300 and 200 K; (d) $Cl + HCl \rightarrow ClH + Cl$ at 200 and 150 K. Coordinates R and r are mass-scaled Jacobi coordinates in atomic units.

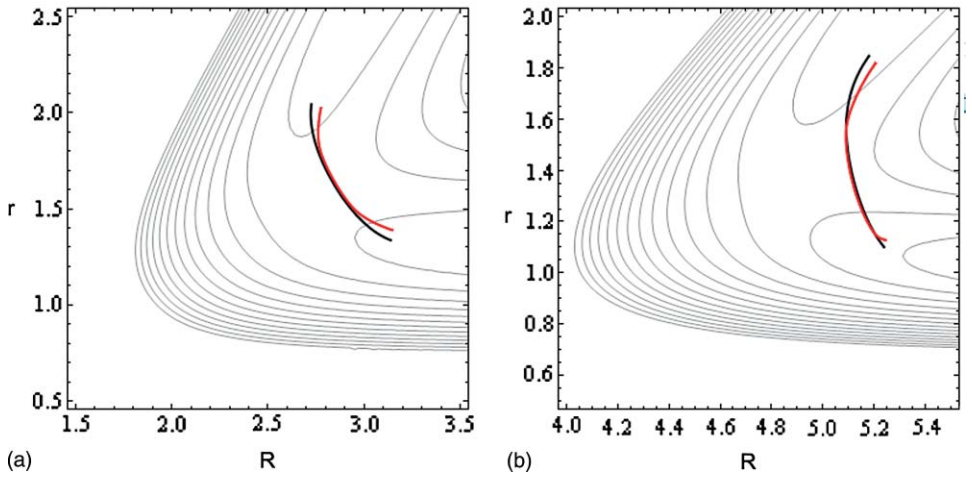

FIG. 3. Instanton trajectories of two semiclassical instanton theories of the present paper: SI1 (black) and SI2 (red). Inset (a) shows instantons for collinear reaction $H + H_2 \rightarrow H_2 + H$ at temperature 300 K, inset (b) shows instantons for collinear reaction $Cl + H_2 \rightarrow ClH + H$ at temperature 200 K. Coordinates R and r are mass-scaled Jacobi coordinates in atomic units.

asymmetric atom transfer reactions. The exact canonical rate constants for these reactions were taken from Ref. 45 with potential energy surface given in Ref. 46. The semiclassical results of SI1 and SI2 instanton approximations

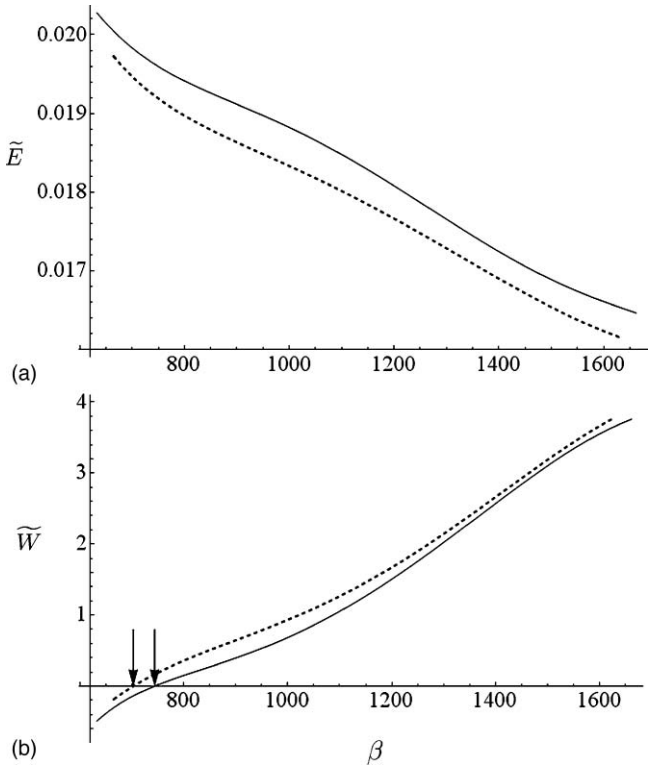

FIG. 4. Energy $\widetilde{E}$ and shortened action $\widetilde{W}$ of $\hbar\beta$-periodic classical trajectory in the effective one-dimensional potential $-\tilde{V}(s)$ as a function of inverse temperature $\beta = 1/\kappa_B T$ for collinear reaction $H + H_2 \rightarrow H_2 + H$ on the Porter–Karplus PES II. Solid lines represent results from SI1 instanton theory, dashed lines represent results from SI2 instanton theory. Arrows indicate the critical temperatures (from left to right): $\widetilde{T}_{c2}$ and $\widetilde{T}_{c1}$, which are the effective critical temperatures of "one-dimensional" instanton theories SI2 and SI1, respectively. Atomic units are used.

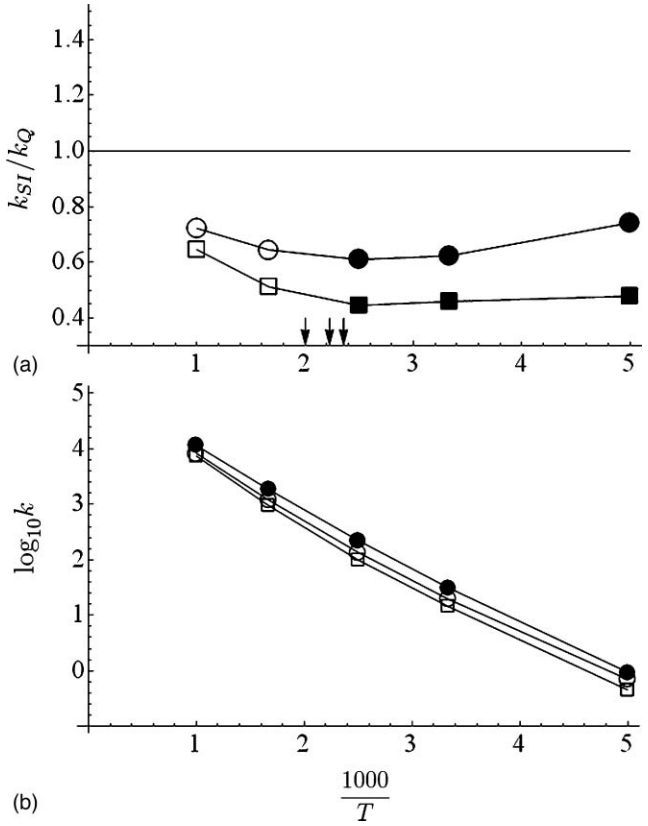

FIG. 5. Canonical rate coefficients for collinear reaction $H + H_2 \rightarrow H_2 + H$. Inset (a): the ratio of semiclassical instanton rate coefficients k_{SI} to exact quantum rate coefficients k_Q, taken from Ref. 45. Semiclassical rate coefficients k_{SI} are calculated within SI1 (squares) and SI2 (circles) approximation using high-temperature (open symbols) expressions (36), (49), and low-temperature (solid symbols) expressions (35), (48). Arrows indicate critical temperatures (from left to right): T_c, $\widetilde{T}_{c2}$, and $\widetilde{T}_{c1}$, which are, respectively, the critical temperature for appearance of classical periodic trajectories on inverted PES, the effective critical temperatures of instanton theory SI2 and that of SI1. Inset (b): absolute values of canonical rate coefficients in units of cm/s; solid circles stand for exact quantum results, open squares and open circles stand for SI1 and SI2 semiclassical instanton results, respectively.

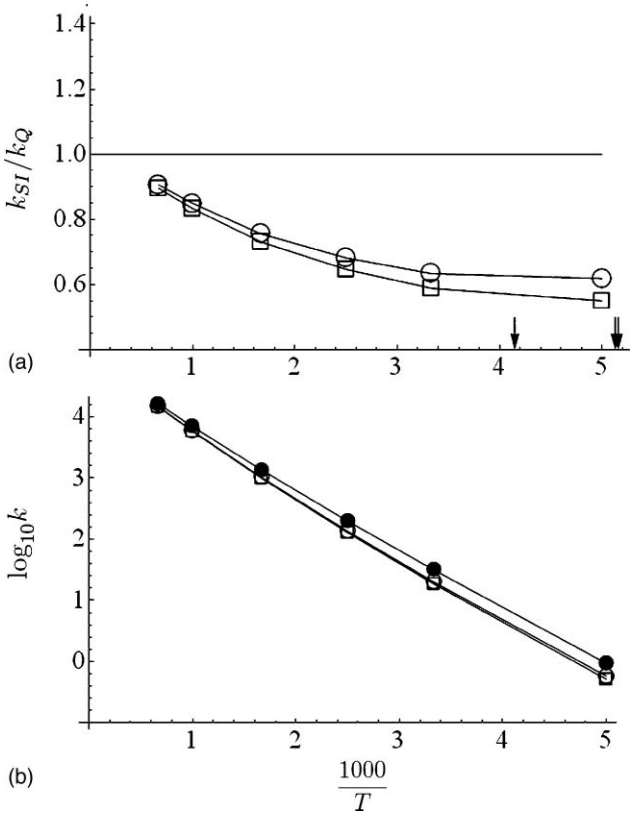

FIG. 6. Canonical rate coefficients for collinear reaction $Cl + D_2 \rightarrow ClD + D$. Labels are the same as in Fig. 5 with exact values k_Q taken from Ref. 45.

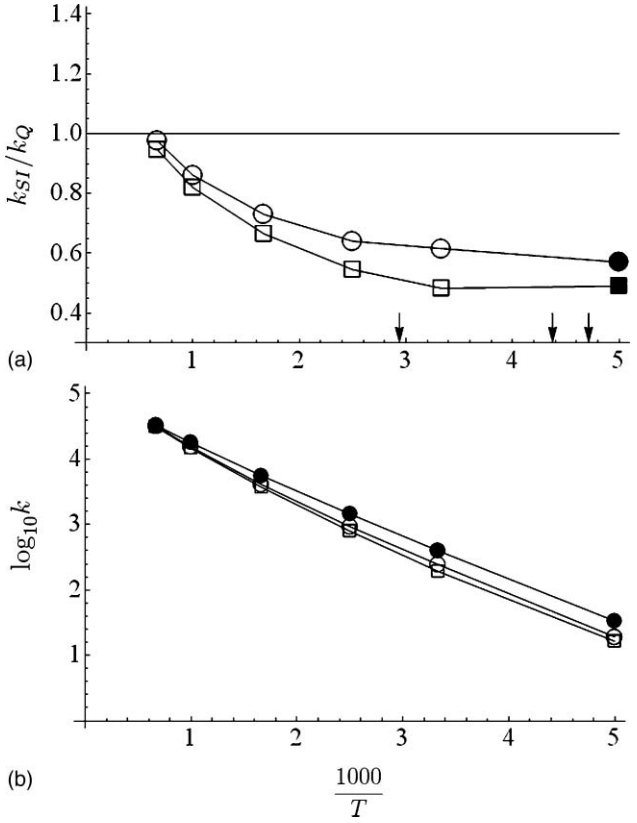

FIG. 7. Canonical rate coefficients for collinear reaction $Cl + H_2 \rightarrow ClH + H$. Labels are the same as in Fig. 5 with exact values k_Q taken from Ref. 45. Arrows indicate critical temperatures (from left to right): T_c, $\widetilde{T}_{c2}$, and $\widetilde{T}_{c1}$.

are given in Figs. 6 and 7. For the reaction with D_2, both SI1 and SI2 results agree within a factor of 1.5 with exact quantum results, while for the reaction with H_2 the agreement is within factors of 2 and 1.5 respectively. The semiclassical instanton results for both reactions coincide with exact quantum results at high temperatures. Examples of instanton trajectories for reaction $Cl + H_2 \rightarrow ClH + H$ at different temperatures are given in Figs. 3(b) and 2(c).

C. H + BrH → HBr + H and D + BrH → DBr + H

Collinear reactions $H + BrH \rightarrow HBr + H$ and $D + BrH \rightarrow DBr + H$ are examples of light-heavy-light atom transfer reactions. We used DIM3C2001 potential surface of Ref. 47 and the exact canonical rate constants from Ref. 48. For heavy-light-heavy reactions we evaluated semiclassical rate constants using the simplest SI1 approximation. SI2 instanton approximation is not expected to contribute any improvement over SI1 approximation due to low variation of zero-point energy of transverse degrees of freedom as seen from Fig. 8. The results of semiclassical SI1 instanton approximation is compared to exact quantum results in Figs. 9 and 10 and observe very good agreement, with almost perfect matching for "heavier" D + BrH reaction.

D. Cl + HCl → ClH + Cl and Cl + DCl → ClD + Cl

Collinear reactions $Cl + HCl \rightarrow ClH + Cl$ and $Cl + DCl \rightarrow ClD + Cl$ are well-known examples of heavy-light-heavy atom transfer reactions. For PES of these reactions we use potential energy surface of Ref. 49 and take exact canonical rate coefficients from Ref. 50. The semiclassical instanton rate coefficients for $Cl + DCl \rightarrow ClD + Cl$ were calculated from the usual expressions (35)–(36) and (48)–(49) and are shown in Fig. 11. Semiclassical instanton

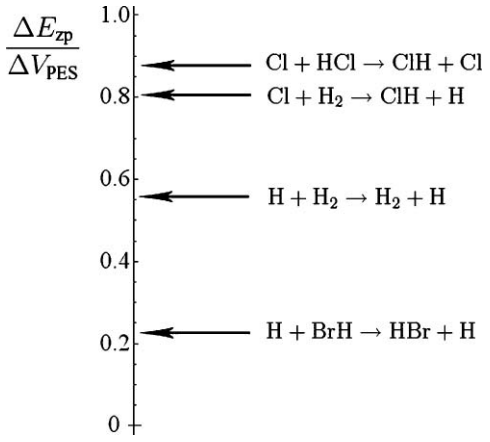

FIG. 8. Ratio of variation in zero-point energy ΔE_{zp} of transverse fluctuations to the variation ΔV_{PES} of one-dimensional instanton potential along the classical periodic trajectory. Once the classical periodic trajectory $\mathbf{x}(\tau)$ is determined on inverted PES, $-V_{PES}$, then $\Delta V_{PES} = \max_\tau V_{PES}(\mathbf{x}(\tau)) - \min_\tau V_{PES}(\mathbf{x}(\tau))$ and $\Delta E_{zp} = [\max_\tau \Omega(\mathbf{x}(\tau)) - \min_\tau \Omega(\mathbf{x}(\tau))]\hbar/2$. The higher the ratio is the greater the difference between the results of SI1 and SI2 instanton theories is expected.

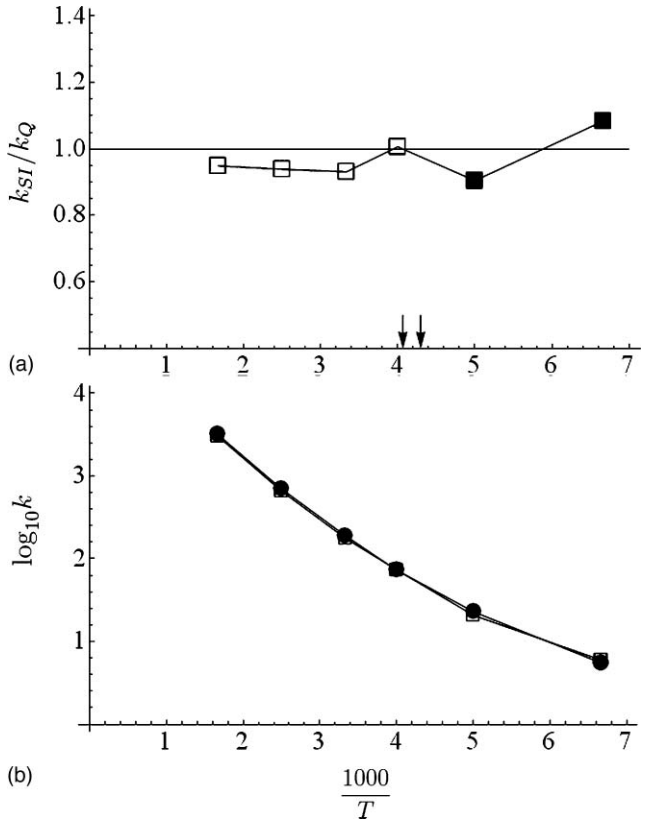

FIG. 9. Canonical rate coefficients for collinear reaction $D + BrH \rightarrow DBr + H$. Labels are the same as in Fig. 5 with exact values k_Q taken from Ref. 48. Arrows indicate critical temperatures (from left to right): T_c, $\widetilde{T}_{c1}$.

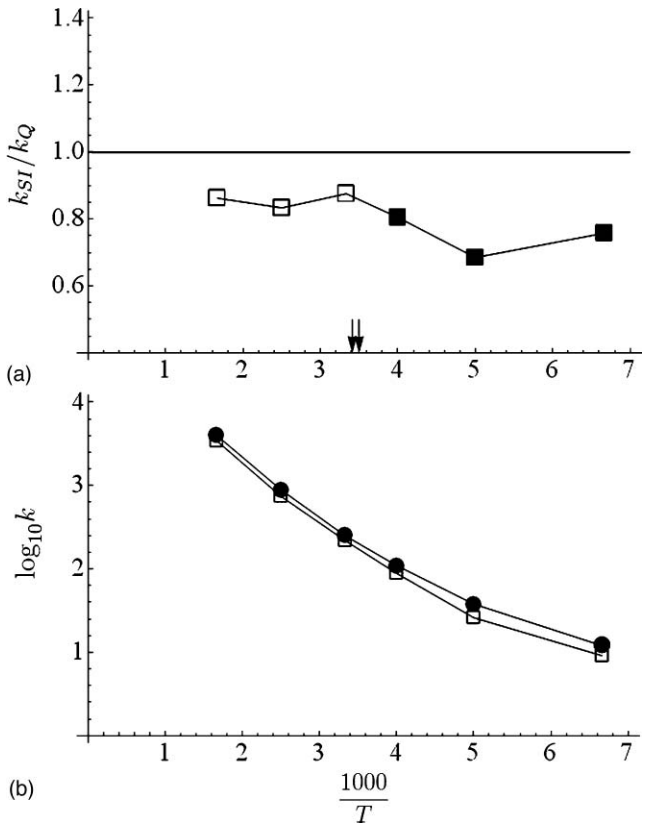

FIG. 10. Canonical rate coefficients for collinear reaction $H + BrH \rightarrow HBr + H$. Labels are the same as in Fig. 5 with exact values k_Q taken from Ref. 48. Arrows indicate critical temperatures (from left to right): T_c, $\widetilde{T}_{c1}$.

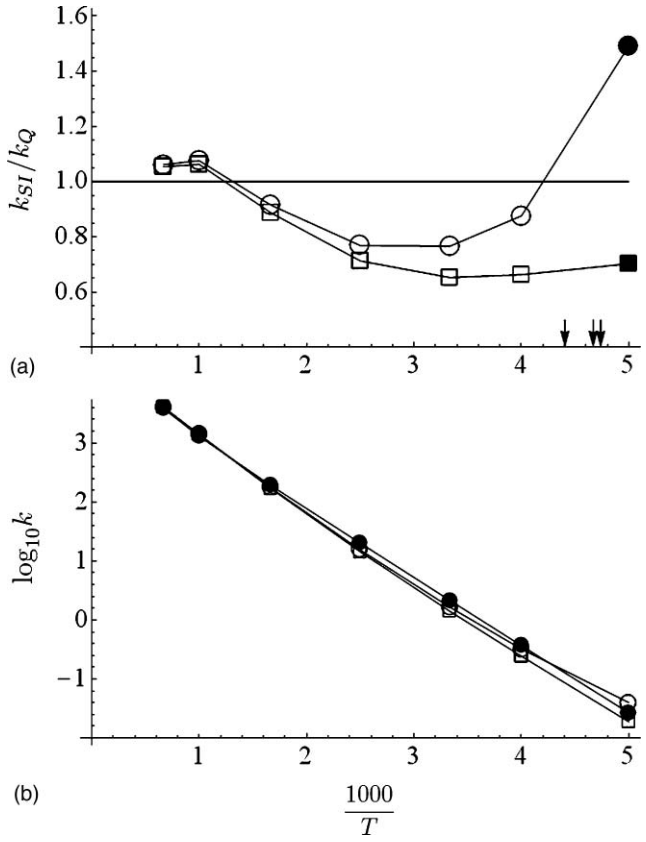

FIG. 11. Canonical rate coefficients for collinear reaction $Cl + DCl \rightarrow ClD + Cl$. Labels are the same as in Fig. 5 with exact values k_Q taken from Ref. 50. Arrows indicate critical temperatures (from left to right): T_c, $\widetilde{T}_{c1}$, and $\widetilde{T}_{c2}$.

rate coefficients agree with exact quantum results within a factor of 1.5 and match exact results at higher temperatures.

Interestingly, the mass-scaled potential energy surfaces of six collinear reactions considered so far, including the one for Cl + DCl reaction, resulted in monotonic functions $\widetilde{E}(\beta)$ and $\widetilde{W}(\beta)$, i.e., for any two instanton trajectories with periods $\hbar\beta_1$ and $\hbar\beta_2$, such that $\beta_1 \le \beta_2$, we always have $\widetilde{E}(\beta_1) \ge \widetilde{E}(\beta_2)$ and $\widetilde{W}(\beta_1) \le \widetilde{W}(\beta_2)$ (see Fig. 4). The latter means that every energy $\widetilde{E}$ generally corresponds to exactly one instanton trajectory of some period $\hbar\beta$ and therefore the parametric dependence $\widetilde{E}(\beta)$ and $\widetilde{W}(\beta)$ produces a well-defined function $\widetilde{W}(\widetilde{E})$, which corresponds to our effective one-dimensional system $\widetilde{V}_b(s)$. Yet, the latter is *not* true for the collinear reaction $Cl + HCl \rightarrow ClH + Cl$. As one can see from the Fig. 12, the functions $\widetilde{E}(\beta)$ and $\widetilde{W}(\beta)$ are not monotonic for collinear reaction ClH + Cl. The latter means that one *cannot* ascribe a simple one-dimensional analog to the reaction ClH + Cl.

For multidimensional systems which do not result in monotonic functions $\widetilde{E}(\beta)$ and $\widetilde{W}(\beta)$ (which we expect to be rare cases) one cannot define a functional dependence $\widetilde{W}(\widetilde{E})$ and therefore the derivations of semiclassical instanton rate coefficients given in Appendix C cannot be performed. To fix this problem we propose a slight modification of the semiclassical rate constant expressions, i.e., we assume that the integral for WKB transmission coefficient $\int \exp(-\widetilde{W}(\widetilde{E}))d\widetilde{E}$ can be understood in a sense $\int \exp(-\widetilde{W}(\beta))\widetilde{E}'(\beta)d\beta$. The latter,

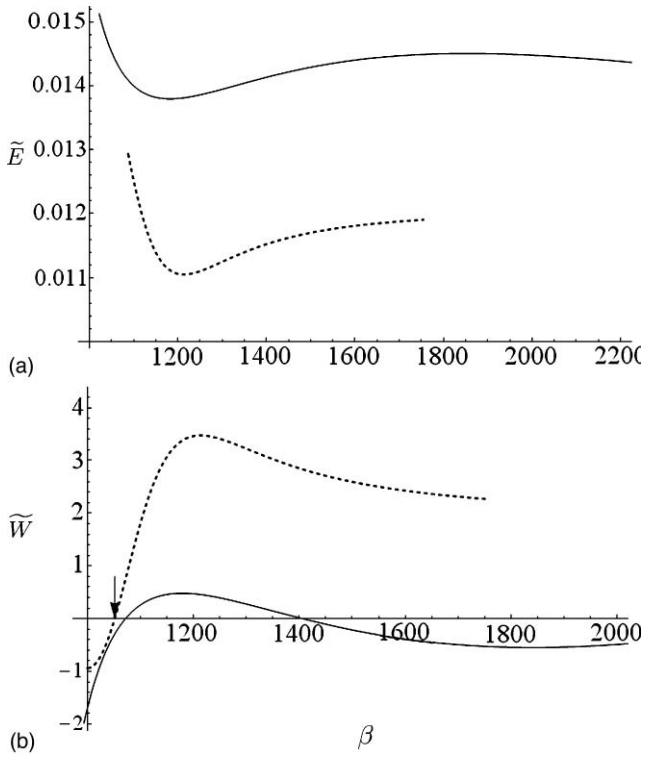

FIG. 12. Energy $\widetilde{E}$ and shortened action $\widetilde{W}$ of $\hbar\beta$-periodic classical trajectory in the effective one-dimensional potential $-\widetilde{V}(s)$ as a function of inverse temperature $\beta = 1/\kappa_B T$ for collinear reaction $Cl + HCl \rightarrow ClH + Cl$ on the Porter–Karplus PES II. Solid lines represent results from SI1 instanton theory, dashed lines represent results from SI2 instanton theory. Arrow indicates the critical temperature $\widetilde{T}_{c2}$, which is the effective critical temperatures of SI2 instanton theory. The critical temperature of SI1 version of instanton theory cannot be identified. Atomic units are used.

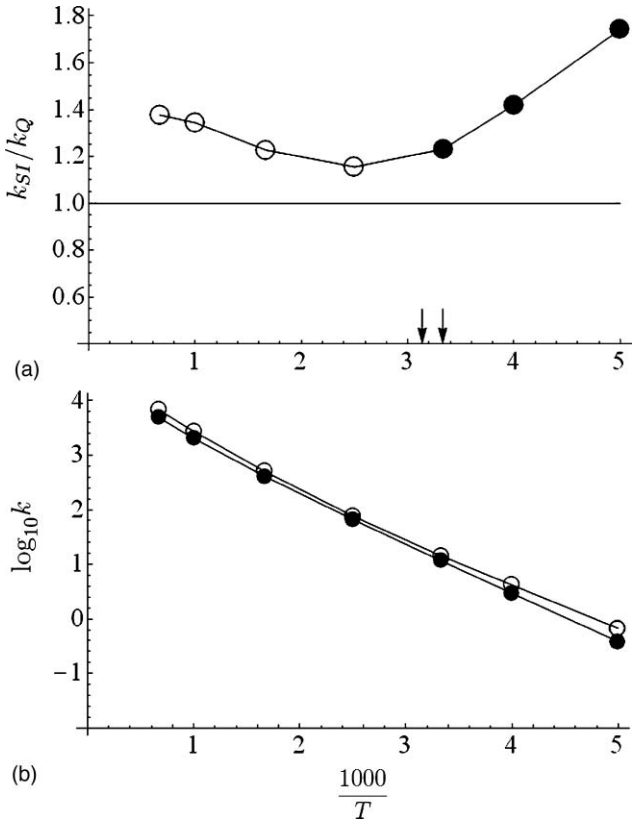

FIG. 13. Canonical rate coefficients for collinear reaction $Cl + HCl \rightarrow ClH + Cl$. Labels are the same as in Fig. 11 with exact values k_Q taken from Ref. 50. Arrows indicate critical temperatures (from left to right): T_c, $\widetilde{T}_{c2}$.

see Appendix C, results in the low-temperature expression for rate coefficient

$$kQ_r = \frac{1}{2\pi\hbar}\int_{-\infty}^{\widetilde{\beta}_c} e^{-\beta\widetilde{E}(\tau)} e^{-\widetilde{W}(\tau)/\hbar}\widetilde{E}'(\tau)d\tau. \quad (56)$$

For the high-temperature rate coefficient expression, we still have the same formula

$$kQ_r = \Delta\sqrt{2\pi}\,\mathrm{erf}(-\Delta)e^{\Delta^2/2}\frac{1}{2\hbar\widetilde{\beta}_c \sin(\pi\beta/\widetilde{\beta}_c)}e^{-\beta\widetilde{V}_0}, \quad (57)$$

$$\Delta = \frac{\beta}{2}\left(\left(\frac{\widetilde{\beta}_c}{\beta}\right)^2 - 1\right)\sqrt{-\widetilde{E}'(\widetilde{\beta}_c)}, \quad (58)$$

except that the derivative $\widetilde{E}'(\widetilde{\beta}_c)$ needs to be determined from the condition of continuity of rate constant k at the critical temperature, i.e., we evaluate k from Eq. (56) at $T = \widetilde{T}_c$, substitute it into Eq. (58) taken at $T = \widetilde{T}_c$ and find $\widetilde{E}'(\widetilde{\beta}_c)$. (For monotonic functions $\widetilde{E}(\beta)$ and $\widetilde{W}(\beta)$ expressions (56) and (57) automatically coincide at $T = \widetilde{T}_c$ as shown in Appendix C).

Using Eqs. (56) and (57) we calculated semiclassical instanton rate coefficients of reaction $Cl + HCl \rightarrow ClH + Cl$ and compared them to exact quantum results in Fig. 13. We used only the SI2 version of semiclassical instanton theory to determine $\widetilde{W}(\beta)$ and $\widetilde{E}(\beta)$ that appear in Eq. (56) since the SI1 instanton theory result in ambiguity in location of critical temperature $\widetilde{T}_c$ (see Fig. 12). An agreement within a factor of 1.8 is observed and improves at higher temperatures.

IX. CONCLUSIONS

In the present paper we revisited the semiclassical instanton approximation and derived corrected semiclassical instanton expressions for the quantum canonical reaction rate coefficients at all temperatures. We specifically addressed the application of the semiclassical instanton theory to multidimensional chemical systems. We have tested the theory on seven collinear atom transfer reactions and found that the accuracy of semiclassical instanton approximation is comparable to the accuracy of modern numerical multidimensional methods.[20,51] Yet, the semiclassical instanton approximation is more transparent analytically, provides simple physical picture of the process of multidimensional tunneling and rigorously recovers the limits of classical transition state theory and the deep tunneling limit of quantum transition state theory.

In the present paper we propose two versions of semiclassical instanton rate theory, SI1 and SI2, discussed in Secs. II–V and VI, respectively. Both theories produced similar results for the tested collinear reactions, yet the results of SI2 approximation are always better than the corresponding results of SI1 approximation. The semiclassical results of SI1 approximation were found to agree with exact results within a factor of 2 or better, while those of SI2 agree with exact

results within a factor of 1.5 or better. The observed accuracy is probably the highest accuracy that can be reached by a semiclassical rate theory developed on a single classical trajectory. The improvement in accuracy of SI2 approximation over SI1 approximation also points out the Gutzwiller approximation as a source of additional error. Within the Gutzwiller approximation the stability parameters λ_n are considered constant and therefore transverse fluctuations do not influence the trajectory of instanton. The latter is generally not true because the zero-point energy of transverse degrees of freedom introduces an additional potential, which depends on the local curvature of PES along the instanton trajectory and is generally not constant. However, the considered examples of collinear reactions revealed that even if the variation of zero-point energy of transverse fluctuations is comparable to the variation of PES along the instanton path (see Fig. 12) the results of SI1 and SI2 theories are comparable. We therefore conclude that slightly more accurate but yet computationally less efficient SI2 approximation of Sec. VI does not lead to considerable improvement of the results of SI1 approximation.

Several other factors may be responsible for the limited accuracy of the present instanton approach. The first one is the assumption of independent quantum fluctuations of the local longitudinal X and transverse $\mathbf{Y}$ degrees of freedom. For a curved instanton path the fluctuations δX and $\delta \mathbf{Y}$ are generally not independent and may influence each other through the instanton's path curvature. However, the transformation from the local curvilinear $\{X, \mathbf{Y}\}$ to the global Cartesian coordinates $\{\mathbf{x}\}$ that was used in Sec. II may automatically incorporate instanton path curvature as shown in Ref. 10, we will explore the effects of instanton path curvature in future publications. The second factor is the effect of anharmonicity. The semiclassical instanton approach assumes quadratic approximation for the transverse to instanton degrees of freedom. To what extent anharmonicity influences the semiclassical instanton results is the subject of future research. From our present analysis of several bimolecular reactions we speculate that the effect of anharmonicity may contribute a factor of up to 1.5 to the semiclassical instanton reaction rate coefficient. Another factor that may limit the accuracy of the semiclassical instanton approach is the effect of rotation and vibration–rotation coupling. Indeed, since in the present paper we considered only collinear systems we have not run into problems associated with rotations. For a general rotating polyatomic molecule, instanton trajectories should satisfy conservation of angular momentum and the appropriate vibrational coordinates for instantons will be then nontrivial curvilinear internal coordinates.[10] We will address these questions in future studies.

The semiclassical instanton theory benefits in many ways from the fact that the problems of Chemical Physics concern mainly near-the-barrier region of potential energy surface. First, it implies sufficiently small instanton trajectories and as a consequence, only a small number of Fourier coefficients to describe these trajectories. Second, since the instanton periods, $\hbar\beta$, are finite, one can easily find stability parameters λ_n along such trajectories. The latter, for instance, is a problem[10] in low temperature Physics, where the instanton periods are infinite.

It is also interesting to note that the imaginary free energy approach used in the present paper does not lead to the recrossing problem[20,52] known in transition state theory for reactions $\mathrm{Cl} + \mathrm{HCl} \rightarrow \mathrm{ClH} + \mathrm{Cl}$ and $\mathrm{Cl} + \mathrm{DCl} \rightarrow \mathrm{ClD} + \mathrm{Cl}$. In particular, the QI approximation of transition state theory[19] observed disagreement[20] with a factor of about 3 between the approximate and quantum results. The latter is thought to be due to multiple recrossings of dividing surface introduced in transition state theory. The imaginary free energy approach does not introduce the concept of dividing surface and is probably the reason for better agreement with exact quantum results for these particular reactions.

We believe that the transparency and simplicity of the present instanton approximation will allow one to develop realistic physical models of atom and charge transfer reactions in complex biological systems as well as to incorporate the effects of dissipation and nonadiabaticity, which have been already developed for one-dimensional systems.

ACKNOWLEDGMENTS

I would like to acknowledge the vital contribution of Professor Rudy Marcus to this paper. His stimulating discussions and encouragement at all stages of the project have insured its progress. I am also pleased to acknowledge the support of the James W. Glanville Fellowship fund, and of the several granting agencies supporting research of the R. A. Marcus group, ONR, NSF, and ARO.

APPENDIX A: CLASSICAL MECHANICS IN IMAGINARY TIME

In this Appendix we review a formulation of classical mechanics in imaginary time.[7,30] The necessity to do so comes from the fact that the Boltzmann operator in the form $e^{-\beta H}$ looks similar to the propagator $e^{-\imath H t}$ if one defines $t = -\imath\beta$. We now define $t = -\imath\tau$ and substitute it into the Hamilton's equations of motion

$$-\frac{d\mathbf{x}}{d(\imath\tau)} = \frac{\mathbf{p}}{m},$$
$$-\frac{d\mathbf{p}}{d(\imath\tau)} = -\frac{\partial V(\mathbf{x})}{\partial \mathbf{x}}. \tag{A1}$$

To keep Hamilton's equations real as well as to keep $\mathbf{x}$ in real domain we define a complex momentum $\overline{\mathbf{p}} = -\imath\mathbf{p}$ and obtain

$$\frac{d\mathbf{x}}{d\tau} = \frac{\overline{\mathbf{p}}}{m},$$
$$\frac{d\overline{\mathbf{p}}}{d\tau} = +\frac{\partial V(\mathbf{x})}{\partial \mathbf{x}}. \tag{A2}$$

One can see that in the coordinates $\mathbf{x}, \overline{\mathbf{p}}$, and τ (hereafter called new coordinates) Hamilton's equations of motion have the same form as in the old $\mathbf{x}, \mathbf{p}, t$ coordinates except that $V(x)$ is flipped now. Energy of the constant-energy system in new coordinates takes the form

$$E = -\frac{\overline{\mathbf{p}}^2}{2m} + V(\mathbf{x}). \tag{A3}$$

We now define new full and shortened actions $\overline{S} = -\imath S$ and $\overline{W} = -\imath W$, respectively, where S and W are the classical full and shortened actions in $\mathbf{x}$, $\mathbf{p}$, t coordinates, to have

$$\begin{aligned}\overline{S} &= -\imath \int \left(\frac{\mathbf{p}^2}{2m} - V(\mathbf{x})\right) dt \\ &= \int \left(\frac{\overline{\mathbf{p}}^2}{2m} + V(\mathbf{x})\right) d\tau, \end{aligned} \tag{A4}$$

$$\begin{aligned}\overline{W} &= -\imath \oint \mathbf{p}\delta\mathbf{x} \\ &= \oint \overline{\mathbf{p}}\delta\mathbf{x}. \end{aligned} \tag{A5}$$

For a one-dimensional system, one can see from Eqs. (A5) and (A3) that $\overline{W} = \int \sqrt{2m(V-E)}dx$ is just a shortened WKB action. From Eqs. (A4)–(A3) and (A2) one can also obtain a helpful relation

$$\overline{S} = \tau E + \overline{W}, \tag{A6}$$

where τ is the total time of a trajectory propagation on the inverted potential. Employing the well-known result that shortened action is stationary for constant-energy motion,[53] i.e., $\delta\overline{W} = 0$, variation of Eq. (A6)

$$\delta\overline{S} = \delta\tau E + \tau\delta E + \frac{\partial\overline{W}}{\partial E}\delta E, \tag{A7}$$

gives two other helpful relations

$$\frac{\partial\overline{W}}{\partial E} = -\tau \tag{A8}$$

and

$$\frac{\partial\overline{S}}{\partial\tau} = E. \tag{A9}$$

APPENDIX B: LAPLACE METHOD FOR APPROXIMATION OF INTEGRALS

Laplace method, which is often called the steepest descent approximation, is a very convenient and widely used method to approximate integrals in the form

$$I(\lambda) = \int_a^b e^{\lambda f(x)} dx, \tag{B1}$$

where $f(x)$ is a function that attains absolute maximum at $x = x_0$ on the interval $[a, b]$. The idea of the method is to Taylor-expand the function $f(x)$ around its maximum x_0 up to a quadratic term

$$f(x) \approx f(x_0) + \frac{1}{2}f''(x_0)(x - x_0)^2, \tag{B2}$$

substitute this expansion into Eq. (B1) and then to take a gaussian integral

$$e^{\lambda f(x_0)} \int_a^b e^{\frac{\lambda}{2}f''(x_0)(x-x_0)^2} dx. \tag{B3}$$

Gaussian integral (B3) is simple if x_0 is far from the boundaries of the interval $[a, b]$, i.e., $a \ll x_0 \ll b$, in that case the limits of integration in Eq. (B3) can be extended to $\pm\infty$, and one obtains the approximation

$$I(\lambda) \approx \sqrt{\frac{2\pi}{-\lambda f''(x_0)}} e^{\lambda f(x_0)}. \tag{B4}$$

In cases when the assumption of $x_0 \ll b$ does not hold (for instance, when the energy spectrum is truncated at the barrier) one should use instead the general form of gaussian integral

$$I(\lambda) \approx \sqrt{\frac{2\pi}{-\lambda f''(x_0)}} e^{\lambda f(x_0)} \mathrm{erf}\left(\sqrt{-\lambda f''(x_0)}(b - x_0)\right), \tag{B5}$$

where

$$\mathrm{erf}(x) = \frac{1}{\sqrt{2\pi}} \int_{-\infty}^{x} e^{-t^2/2} dt. \tag{B6}$$

APPENDIX C: FLUX OVER ONE-DIMENSIONAL BARRIER

In this Appendix we follow the derivations of the Ref. 2. For temperatures lower than critical, T_c, the flux f over one-dimensional barrier $V(x)$ of height V_0 is given by the product of the free particle flux $1/2\pi\hbar$ and the WKB transmission coefficient

$$f = \frac{1}{2\pi\hbar} \int_{-\infty}^{V_0} dE e^{-\beta E} e^{-W(E)/\hbar}. \tag{C1}$$

The integral is truncated at $E = V_0$, since for the temperatures of interest, i.e., $T < T_c$, contributions of $E > V_0$ are negligible. One then Taylor expands the shortened action $W(E)$ around the energy E_0 that corresponds to the classical instanton trajectory of period $\hbar\beta$ on the inverted potential $-V(x)$, i.e., one expands $W(E)$ around the point E_0 such that $W'(E_0) = -\hbar\beta$ (see Appendix A)

$$\begin{aligned} W(E) &\approx W(E_0) + W'(E_0)(E - E_0) + \frac{1}{2}W''(E_0)(E - E_0)^2 \\ &= S_0 - \hbar\beta E + \frac{1}{2}W''(E_0)(E - E_0)^2, \end{aligned} \tag{C2}$$

where $S_0 = W(E_0) + \hbar\beta E_0$ is the full classical action from Appendix A. Substituting Eq. (C2) into Eq. (C1) and taking simple gaussian integral one obtains

$$f = \sqrt{\frac{-E'(\beta)}{2\pi\hbar^2}} e^{-S_0/\hbar} \mathrm{erf}\left[\frac{V_0 - E_0}{\sqrt{-E'(\beta)}}\right], \tag{C3}$$

where $E'(\beta) \equiv dE/d\beta = -\hbar/W''(E_0)$ (see Appendix A).

For temperatures at and above the crossover temperature T_c the flux over the one dimensional barrier is controlled mainly by the region near the barrier top $V(x_0) = V_0$. Expanding the barrier $V(x)$ in Taylor series to the fourth power in x and representing x in terms of Fourier series, one can perform rigorous evaluation of path integral[2] which results in

$$f = \mathrm{Corr}(\Delta) f_{pb}, \tag{C4}$$

where

$$f_{pb} = \frac{1}{2\pi\hbar\beta} \frac{\hbar\beta\omega_b/2}{\sin(\hbar\beta\omega_b/2)} \exp(-\beta V_0) \tag{C5}$$

is the parabolic barrier reactive flux and

$$\mathrm{Corr}(\Delta) = \Delta\sqrt{2\pi}\,\mathrm{erf}(-\Delta)e^{\Delta^2/2}, \tag{C6}$$

with

$$\Delta = \frac{\beta}{2}\left(\left(\frac{\beta_c}{\beta}\right)^2 - 1\right)\sqrt{-E'(\beta_c)}. \tag{C7}$$

is the correction factor due to anharmonicity of the potential barrier near its top. Here β_c stands for the inverse critical temperature $\beta_c = 1/\kappa_B T_c = 2\pi/\omega_b\hbar$ and ω_b is the harmonic frequency of the barrier.

It is easy to show now that at temperatures in the vicinity of T_c, expressions (C3) and (C4) coincide. Indeed, for values of β close to β_c we have

$$\begin{aligned}\Delta &\approx (\beta_c - \beta)\sqrt{-E'(\beta_c)},\\ f_{pb} &= \frac{1}{2\hbar\beta_c}\frac{1}{\sin(\pi\beta/\beta_c)}\exp(-\beta V_0),\\ &\approx \frac{1}{2\pi\hbar(\beta_c - \beta)}\exp(-\beta V_0),\end{aligned} \tag{C8}$$

and therefore Eq. (C4) reads

$$f = \sqrt{\frac{-E'(\beta_c)}{2\pi\hbar^2}}\mathrm{erf}[(\beta - \beta_c)\sqrt{-E'(\beta_c)}]e^{-\beta V_0 - (\beta-\beta_c)^2 E'(\beta_c)/2}. \tag{C9}$$

Using Taylor expansions $E(\beta) = E(\beta_c) + E'(\beta_c)(\beta - \beta_c)$, $S(\beta) = S(\beta_c) + S'(\beta_c)(\beta - \beta_c) + S''(\beta_c)(\beta - \beta_c)^2/2$ with $E(\beta_c) = V_0$, $S(\beta_c) = W(\beta_c) + \hbar\beta_c E(\beta_c) = \hbar\beta_c V_0$ and $dS/d(\beta\hbar) = E(\beta)$ (see Appendix A) Eq. (C9) reads

$$f = \sqrt{\frac{-E'(\beta_c)}{2\pi\hbar^2}}e^{-S(\beta)/\hbar}\mathrm{erf}\left[\frac{V_0 - E(\beta)}{\sqrt{-E'(\beta_c)}}\right], \tag{C10}$$

and is the same as Eq. (C3) at $\beta = \beta_c$.

[1] I. Affleck, Phys. Rev. Lett. **46**, 388 (1981).
[2] J. Cao and G. A. Voth, J. Chem. Phys. **105**, 6856 (1996).
[3] H. Grabert and U. Weiss, Phys. Rev. Lett. **53**, 1787 (1984).
[4] P. Hanggi, J. Stat. Phys. **42**, 105 (1986).
[5] R. A. Marcus and M. E. Coltrin, J. Chem. Phys. **67**, 2609 (1977).
[6] D. G. Truhlar and B. C. Garrett, Ann. Rev. Phys. Chem. **35**, 159 (1984).
[7] W. H. Miller, J. Chem. Phys. **62**, 1899 (1975).
[8] V. A. Benderskii, D. E. Makarov, and P. G. Grinevich, Chem. Phys. **170**, 275 (1993).
[9] Z. Smedarchina, W. Siebrand, and M. Z. Zgierski, J. Chem. Phys. **103**, 5326 (1995).
[10] G. V. Mil'nikov and H. Nakamura, J. Chem. Phys. **115**, 6881 (2001).
[11] G. V. Mil'nikov and H. Nakamura, Phys. Chem. Chem. Phys. **10**, 1374 (2008).
[12] A. O. Caldeira and A. J. Legget, Phys. Rev. Let. **46**, 211 (1981).
[13] A. O. Caldeira and A. J. Legget, Ann. Phys. **149**, 374 (1983).
[14] H. Grabert, U. Weiss, and P. Hanggi, Phys. Rev. Lett. **52**, 2193 (1984).
[15] G. Mills, G. K. Schenter, D. E. Makarov, and H. Jonsson, Chem. Phys. Lett. **278**, 91 (1997).
[16] S. Andersson, G. Nyman, A. Arnaldsson, U. Manthe, and H. Jonsson, J. Phys. Chem. A, **113**, 4468 (2009).
[17] J. O. Richardson and S. C. Althorpe, J. Chem. Phys. **131**, 214106 (2009).
[18] S. Chapman, B. C. Garrett, and W. H. Miller, J. Chem. Phys. **63**, 2710 (1975).
[19] W. H. Miller, Y. Z. M. Ceotto, and S. Yang, J. Chem. Phys. **119**, 1329 (2003).
[20] M. Ceotto and W. H. Miller, J. Chem. Phys. **120**, 6356 (2004).
[21] A. A. Stuchebrukhov, J. Chem. Phys. **95**, 4258 (1991).
[22] V. I. Goldanskii, L. I. Trakhtenberg, and V. N. Fleurov, *Tunneling Phenomena in Chemical Physics* (Gordon and Beach Science Publishers, New York, London, Paris, Montreux, Tokyo, Melbourne, 1988).
[23] G. Gamow, Z. Phys. **51**, 4931 (1928).
[24] U. Weiss, *Quantum Dissipative Systems* (World Scientific, Singapore, 2008).
[25] T. Seideman and W. H. Miller, J. Chem. Phys. **95**, 1768 (1991).
[26] C. D. Schwieters and G. A. Voth, J. Chem. Phys. **108**, 1055 (1998).
[27] V. A. Benderskii, V. I. Goldanskii, and D. E. Makarov, Chem. Phys. **154**, 407 (1990).
[28] V. A. Benderskii and D. E. Makarov, Phys. Lett. A **161**, 535 (1992).
[29] R. P. Feynman, *Statistical Mechanics* (W. A. Benjamin Inc., Reading, 1972).
[30] W. H. Miller, J. Chem. Phys. **55**, 3146 (1971).
[31] M. C. Gutzwiller, J. Math. Phys. **12**, 343 (1971).
[32] V. A. Benderskii, P. G. Grinevich, D. E. Makarov, and D. L. Pastur, Chem. Phys. **161**, 51 (1992).
[33] C. G. Callan and S. Coleman, Phys. Rev. D **16**, 1762 (1977).
[34] L. D. Landau and E. M. Lifschitz, *Quantum Mechanics: Non-relativistic Theory* (Elsevier Science, Oxford, 1991).
[35] E. Wigner, Z. Phys. Chem. Abt. B **19**, 203 (1932).
[36] W. H. Miller, J. Chem. Phys. **61**, 1823 (1974).
[37] A. Kuppermann, J. Phys. Chem. **83**, 171 (1979).
[38] G. A. Voth, D. Chandler, and W. H. Miller, J. Chem. Phys. **91**, 7749 (1989).
[39] E. Pollak and J. L. Liao, J. Chem. Phys. **108**, 2733 (1998).
[40] V. K. Babamov and R. A. Marcus, J. Chem. Phys. **74**, 1790 (1981).
[41] E. J. Heller, Phys. Rev. Lett. **53**, 1515 (1984).
[42] C. D. Schwieters and G. A. Voth, J. Chem. Phys. **108**, 1055 (1997).
[43] R. D. Coalson, D. L. Freeman, and J. D. Doll, J. Chem. Phys. **85**, 4567 (1986).
[44] R. N. Porter and M. Karplus, J. Chem. Phys. **40**, 1105 (1964).
[45] B. C. Garrett and D. G. Truhlar, J. Phys. Chem. **83**, 1079 (1979).
[46] M. Baer, Mol. Phys. **27**, 1429 (1974).
[47] R. J. Duchovic, Y. L. Volobuev, G. C. Lynch, A. W. Jasper, D. G. Truhlar, T. C. Allison, A. F. Wagner, B. C. Garrett, J. Espinosa-García, J. C. Corchado, POTLIB http://comp.chem.umn.edu/potlib.
[48] D. C. Clary, B. C. Garrett, and D. G. Truhlar, J. Chem. Phys. **78**, 777 (1973).
[49] D. K. Bondi, J. N. L. Connor, J. Manz, and J. Romelt, J. Mol. Phys. **50**, 467 (1983).
[50] D. K. Bondi, J. N. L. Connor, B. C. Garrett, and D. G. Truhlar, J. Chem. Phys. **78**, 5981 (1983).
[51] R. Collepardo-Guevara, Y. V. Suleimanov, and D. E. Manolopoulos, J. Chem. Phys. **130**, 174713 (2009).
[52] J. W. Tromp and W. H. Miller, Faraday Discuss. Chem. Soc. **84**, 441 (1987).
[53] L. D. Landau and E. M. Lifschitz, *Mechanics* (Pergamon, Oxford, New York, 1989).